

A new pterosaur from the Middle Jurassic of Skye, Scotland and the early diversification of flying reptiles

Elizabeth Martin-Silverstone, David M. Unwin, Andrew R. Cuff, Emily E. Brown, Lu Allington-Jones & Paul M. Barrett

To cite this article: Elizabeth Martin-Silverstone, David M. Unwin, Andrew R. Cuff, Emily E. Brown, Lu Allington-Jones & Paul M. Barrett (05 Feb 2024): A new pterosaur from the Middle Jurassic of Skye, Scotland and the early diversification of flying reptiles, Journal of Vertebrate Paleontology, DOI: [10.1080/02724634.2023.2298741](https://doi.org/10.1080/02724634.2023.2298741)

To link to this article: <https://doi.org/10.1080/02724634.2023.2298741>



© 2024. Elizabeth Martin-Silverstone, David M. Unwin, Andrew R. Cuff, Emily E. Brown, Lu Allington-Jones, Paul M. Barrett.



View supplementary material [↗](#)



Published online: 05 Feb 2024.



Submit your article to this journal [↗](#)



Article views: 3836



View related articles [↗](#)



View Crossmark data [↗](#)

A NEW PTEROSAUR FROM THE MIDDLE JURASSIC OF SKYE, SCOTLAND AND THE EARLY DIVERSIFICATION OF FLYING REPTILES

ELIZABETH MARTIN-SILVERSTONE, *¹ DAVID M. UNWIN, ² ANDREW R. CUFF, ³ EMILY E. BROWN, ^{4,5}
LU ALLINGTON-JONES, ⁶ and PAUL M. BARRETT ⁴

¹Bristol Palaeobiology Group, School of Earth Sciences, University of Bristol, Life Sciences Building, 24 Tyndall Avenue, Bristol BS8 1TQ, U.K., liz.martin@bristol.ac.uk;

²Centre for Palaeobiology and Biosphere Evolution and School of Museum Studies, University of Leicester, University Road, Leicester LE1 7RH, U.K., dmu1@leicester.ac.uk;

³Human Anatomy Resource Centre, University of Liverpool, Sherrington Building, Ashton Street, Liverpool L69 3GE, U.K., andrew.cuff@liverpool.ac.uk;

⁴Fossil Reptiles, Amphibians, and Birds Section, Natural History Museum, Cromwell Road, London SW7 5BD, U.K., emily.brown2@nhm.ac.uk;

⁵School of Geography, Earth & Environmental Sciences, University of Birmingham, Edgbaston, Birmingham B15 2TT, U.K., emily.brown2@nhm.ac.uk;

⁶Conservation Centre, Natural History Museum, Cromwell Road, London SW7 5BD, U.K., l.allington-jones@nhm.ac.uk; p.barrett@nhm.ac.uk

ABSTRACT—The Middle Jurassic was a critical time in pterosaur evolution, witnessing the appearance of major morphological innovations that underpinned successive radiations by rhamphorhynchids, basally branching monofenestratans, and pterodactyloids. Frustratingly, this interval is particularly sparsely sampled, with a record consisting almost exclusively of isolated fragmentary remains. Here, we describe new material from the Bathonian-aged Kilmaluag Formation of Skye, Scotland, which helps close this gap. *Ceoptera evansae* (gen. et sp. nov.) is based on a three-dimensionally preserved partial skeleton, which represents one of the only associated Middle Jurassic pterosaurs. *Ceoptera* is among the first pterosaurs to be fully digitally prepared, and μ CT scanning reveals multiple elements of the skeleton that remain fully embedded within the matrix and otherwise inaccessible. It is diagnosed by unique features of the pectoral and pelvic girdle. The inclusion of this new Middle Jurassic pterosaur in a novel phylogenetic analysis of pterosaur interrelationships provides additional support for the existence of the controversial clade Darwinoptera, adding to our knowledge of pterosaur diversity and evolution.

<http://zoobank.org/urn:lsid:zoobank.org:pub:445D89B4-1912-45CF-AB85-7FCAA22186F7>

SUPPLEMENTARY FILES—Supplementary files are available for this article for free at www.tandfonline.com/UJVP

Citation for this article: Martin-Silverstone, E. M., Unwin, D. M., Cuff, A. R., Brown, E. E., Allington-Jones, L., & Barrett, P. M. (2024) A new pterosaur from the Middle Jurassic of Skye, Scotland and the early diversification of flying reptiles. *Journal of Vertebrate Paleontology*. <https://doi.org/10.1080/02724634.2023.2298741>

Submitted: December 22, 2022

Revisions received: November 17, 2023

Accepted: December 12, 2023

INTRODUCTION

Pterosaurs first appear during the Late Triassic and persist through to the K-Pg extinction (Barrett et al., 2008; Unwin, 2005; Witton, 2013). The clade includes taxa that fall into three principal morphotypes: ‘rhamphorhynchoids,’ a paraphyletic group of Late Triassic–Late Jurassic basally branching forms; pterodactyloids, a large clade of highly derived Late Jurassic to end-Cretaceous taxa; and ‘darwinopterans,’ Middle–Late Jurassic early-branching monofenestratans that appear to be intermediate between the other morphotypes (Lü et al., 2010). Darwinopterans have been interpreted as a paraphyletic group directly transitional to Pterodactyloidea (Lü et al., 2010), but the unity or otherwise of this clade, and the relationships of the taxa included within it, are controversial, undermining attempts

*Corresponding author.

© 2024, Elizabeth Martin-Silverstone, David M. Unwin, Andrew R. Cuff, Emily E. Brown, Lu Allington-Jones, Paul M. Barrett.

This is an Open Access article distributed under the terms of the Creative Commons Attribution-NonCommercial-NoDerivatives License (<http://creativecommons.org/licenses/by-nc-nd/4.0/>), which permits non-commercial re-use, distribution, and reproduction in any medium, provided the original work is properly cited, and is not altered, transformed, or built upon in any way. The terms on which this article has been published allow the posting of the Accepted Manuscript in a repository by the author(s) or with their consent.

Color versions of one or more of the figures in the article can be found online at www.tandfonline.com/ujvp.

to understand pterosaur evolutionary history (e.g., Wang et al., 2009, 2010, 2017).

The majority of pterosaur remains have been recovered from a handful of Mesozoic Konservat Lagerstätten, which are irregularly distributed in time and space (Barrett et al., 2008; Butler et al., 2009, 2013; Dean et al., 2016; Sullivan et al., 2014; Unwin, 2001; Upchurch et al., 2015; Wellnhofer, 1991; Zhou & Wang, 2010). While Lagerstätten have played a critical role in understanding pterosaur anatomy, functional morphology, and reproduction (Unwin, 2005; Wellnhofer, 1991; Witton, 2013), the potentially detailed insights they give into pterosaur evolutionary history can be biased, misleading, and difficult to interpret. For example, apparent peaks in pterosaur taxonomic diversity during the Late Jurassic (Sullivan et al., 2014; Wellnhofer, 1991; Witton, 2013) and mid-Early Cretaceous (Wellnhofer, 1991; Witton, 2013; Zhou & Wang, 2010) likely reflect the occurrence of multiple Lagerstätten in these intervals, rather than a true diversity signal (Butler et al., 2009, 2013; Dean et al., 2016).

This ‘Lagerstätten effect’ is exacerbated by the paucity of pterosaur finds in the temporal gaps between these windows of exceptional preservation, with the late Early–Middle Jurassic pterosaur fossil record, an interval of almost 20 Ma, being particularly poorly sampled (Barrett et al., 2008; Butler et al., 2009, 2013; Dean et al., 2016; Wellnhofer, 1991). The Taynton Limestone Formation (including the ‘Stonesfield Slates’) of Oxfordshire, U.K., has yielded the most abundant remains, but the bones from this unit are disarticulated, isolated, and often fragmentary, frustrating attempts to determine the species-richness of this assemblage (O’Sullivan & Martill, 2018). Other isolated remains have been reported from elsewhere in the Middle Jurassic of England (Oxford Clay; Barrett et al., 2008) and Scotland, which recently yielded *Dearc*, a three-dimensionally preserved, articulated rhamphorhynchine, and the proximal end of a tibia associated with caudal elements (Jagielska et al., 2022, 2023), as well as important records from Kyrgyzstan, Mongolia, and China (Barrett et al., 2008). Moreover, several important deposits thought to have been of Middle Jurassic age have since been re-dated: the Cañadón Asfalto Formation (Argentina), which yielded *Allkaruen* (Codorníu et al., 2016), is now considered to be late Lower Jurassic (Cúneo et al., 2013) while the Tiaojishan Formation (NE China), which includes rhamphorhynchines, scaphognathines, anurognathids, darwinopterans, and basally branching pterodactyloids, has been dated as lowermost Upper Jurassic (Liu et al., 2012; Xu et al., 2016).

The rarity of Middle Jurassic pterosaurs and their incompleteness (only *Dearc*, a few associated remains of a second indeterminate pterosaur, also from Scotland [Jagielska et al., 2022, 2023], and a possible ?anurognathid from Mongolia [Bakhurina & Unwin, 1995] are known from multiple elements) severely hinders attempts to understand early pterosaur evolution. This problem is reflected in the lack of congruence between recently published pterosaur phylogenies, with little agreement on the compositions and/or likely times of origin of key clades such as Monofenestrata, Darwinoptera, and Pterodactyloidea (Baron, 2020; Dalla Vecchia, 2022; Jagielska et al., 2022; Wei et al., 2021; Zhou et al., 2017). The recovery of associated skeletons, complete or otherwise, of Middle Jurassic pterosaurs is critical for resolving these issues and generating a clearer picture of pterosaur evolutionary history. Here, we describe a new, three-dimensionally preserved, partial pterosaur skeleton from the Middle Jurassic (Bathonian: ~168.3–166.1 Ma) of the Isle of Skye, Scotland. This is only the fourth associated skeleton of a Middle Jurassic pterosaur to be discovered to date.

DISCOVERY AND GEOLOGIC BACKGROUND

The new specimen, NHMUK PV R37110, was found on the north side of Glen Scaladal at Cladach a’Ghlinne, a small

beach that forms part of the coastline of Loch Scavaig, on the Strathaird Peninsula, Isle of Skye, Scotland, U.K.

The area is a Site of Special Scientific Interest (SSSI), which is administered by Scottish Natural Heritage (formerly Scottish Nature), and the land is owned by the John Muir Trust: fieldwork and collection permits were obtained from both organizations and are on file at the Natural History Museum, London. Collection from the cliff faces is not permitted at this locality, but permission was granted to collect from fallen blocks on the wavecut platform.

The specimen was found partially exposed as a scatter of thin-walled bones on a large boulder situated a few meters from the cliff face at the northern-most edge of the beach (close to the small headland that separates Cladach a’Ghlinne from Camasunary Bay). The specimen was collected in several pieces using hand tools and a small angle-grinder and was reconstructed in the Conservation Centre of the NHMUK (see ‘Preparation,’ below).

The vertebrate-bearing horizons at this locality pertain to the Kilmaluag Formation (formerly the ‘Ostracod Limestone’) of the Great Estuarine Group, which crops out in several areas on Skye, Muck, and Eigg, but reaches its maximum thickness (up to 25 m) on the Strathaird Peninsula (Andrews, 1985; Barron et al., 2012; Harris & Hudson, 1980; Panciroli et al., 2020). Most of the vertebrate material known from the formation comes from the vicinity of Cladach a’Ghlinne (reviewed in Evans et al., 2006; Panciroli et al., 2020; White & Ross, 2020). The formation consists of a series of interbedded mudstones and limestones: the vertebrate remains come from the ‘Vertebrate Beds’ (or Beds 9 and 10) of Andrews (1985) and are usually found in mudstone facies. Paleocene volcanic activity emplaced several dykes at Cladach a’Ghlinne, which partially metamorphosed the sediments so that although composed of mudstone they are very hard and difficult to excavate. Paleontological, sedimentological, and geochemical evidence suggests that the Kilmaluag Formation represents a series of freshwater to low-salinity environments that are often interpreted as a closed lagoonal system that fluctuated in depth and extent (Andrews, 1985; Panciroli et al., 2020). Biostratigraphic correlations place the Kilmaluag Formation within the *retrocostatium* Zone of the upper Bathonian (Middle Jurassic) (Barron et al., 2012), ~167.5–166.1 Ma (Walker & Geissman, 2022).

Cladach a’Ghlinne has yielded a rich fauna of macro- and microvertebrate remains, including hybodont sharks, osteichthyan, a ?coelacanth, caudate and albanerpetontid lissamphibians, turtles, lepidosauromorphs, choristoderes, crocodylians, non-avian dinosaurs, and a variety of mammaliaforms (reviewed in Evans et al., 2006; Panciroli et al., 2020; White & Ross, 2020). Isolated pterosaur teeth have been reported from the locality but remain undescribed (Evans et al., 2006).

METHODS

Preparation

Preparation of the pterosaur was challenging, as the density and hardness of the matrix, combined with the extreme fragility and fragmentary nature of the bones, made the specimen unsuitable for mechanical preparation. Acetic acid preparation was the obvious choice for this material, but the limestone had undergone contact metamorphism, leading to uneven hardness and acid resistance.

The blocks were first rinsed with industrial methylated spirit, to remove dust and cutting-tool slurry, and the surfaces were cleaned using air-abrasive to remove carbonate deposits. The blocks were then oriented, the associated surfaces and breaks marked with permanent ink, aligned using modeling clay, adhered together with Paraloid B72 in acetone (Davidson & Brown, 2012), and allowed to cure for 4 days. The undersides

of the blocks were then coated in silicone rubber and supported by a cradle jacket of polyester resin and fiberglass (all resistant to acetic acid). This facilitated handling of the blocks as a single unit and prevented uncontrolled dissolution of their undersides during immersion (Toombs & Rixon, 1959). Application of 10% acetic acid for 48-h immersions was required to soften 1–2 mm of the most resistant areas of metamorphosed limestone. 2.5% w/v precipitated calcium phosphate was added to the acid bath to reduce the solution of phosphate from the fossil material (Lindsay, 1995). This high strength acid had undesirably severe effects on softer sections of the matrix, causing undercuts and pockets to develop. This was successfully combated using local barriers: Synocryl 9123s for the bones and surrounding matrix (Lindsay, 1986; which has since been replaced with Synocryl 9122x; Graham & Allington-Jones, 2015), and microcrystalline wax for larger areas of matrix where undercuts began to develop (Toombs & Rixon, 1959).

Following each acid immersion, the blocks were rinsed in running water for 6 days to remove excess acid and calcium acetate salts (Lindsay, 1995) before mechanical removal of the softened layer with a brush and low-pressure water jet. The block was then dried in an oven for 5 h at 50°C to limit crystal growth. Once dry it was photographed and treated with barrier materials where necessary. The acid immersion, rinsing, oven drying, photography, and masking process was repeated 29 times over the course of 12 months. Any fragments that became detached were labelled and their original location was annotated on photographs. After treatment the rubber and resin jacket was removed and a supporting mount was created using Epopast 400 epoxy laminating paste, lined with Plasta-zote® LD45 foam, and the specimen was housed in an acid-free cardboard box.

CT-scanning and Visualization

In order to visualize all of the preserved remains, including elements that remain fully encased in matrix, microcomputed tomographic (μ CT) scanning of the specimen was performed. An initial exploratory scan was completed at the Natural History Museum Computed Tomography Facility. The final scans that form the basis for our descriptive work were performed at the University of Bristol in the XTM Facility of the School of Earth Sciences using a Nikon XTH 225ST X-ray tomography scanner. Scanning settings and parameters are as follows: (1) all blocks were scanned using a 2 mm copper filter and at 8 frames per projection unless stated otherwise; (2) block A, scanned once using a reflection rotating target to a voxel size of 84.3 μ m (224 kV, 357 μ A, 1415 ms exposure, 3141 projections); (3) block B, scanned twice, first using a reflection target to a voxel size of 80.5 μ m (224 kV, 298 μ A, 2000ms exposure, 3141 projections), and second using a reflection rotating target with a 3 mm copper filter to a voxel size of 35.3 μ m, to zoom into a thicker region that was difficult to visualize in the first scan (222 kV, 205 μ A, 2829 ms exposure, 2850 projections); and (4) block C, scanned once using a reflection target to a voxel size of 64.4 μ m (222 kV, 210 μ A, 1415 ms exposure, 3141 projections, one frame per projection).

Segmentation and visualization of surfaces was performed using Avizo Lite v. 9.5 (ThermoFisher Scientific), following standard procedures (Lautenschlager, 2016, 2017). Elements were grouped into vertebrae, forelimb, hind limb, metatarsal/metacarpal, unknown fragments, and identified bone groups. Colors were chosen using the Okabe and Ito Color Universal Design palette (<https://jfly.uni-koeln.de/color/>). Contrast in some areas was poor making segmentation slow and difficult. This was further complicated by pyrite that frequently infilled bones and caused numerous scanning artifacts (Supplementary Material 1, Fig. S1). The CT-scans and .stl files of the segmented materials of each block

can be downloaded from Morphosource (with downloads controlled by the NHMUK, Project ID 397673).

Phylogenetic Analysis

A phylogenetic analysis was conducted on a pterosaur data matrix consisting of 69 taxa (67 pterosaurs and two outgroups: *Euparkeria* and *Herrerasaurus*) and 136 osteological characters (see Supplementary Material S1, section 2 for character list and Supplementary Material S2 and S3 for data matrices in TNT and NEXUS formats). Taxon selection focused on basally branching monofenestrates, and all named taxa that have been allied with or included in this group were incorporated. We also included a comprehensive sample of early-branching (non-monofenestratan) pterosaurs, putative early pterodactyls (*Douzhanopterus* and *Rhamphodactylus*), and a representative sample of pterodactyls. Characters and their character states were compiled primarily from Lü et al. (2010), but also from Andres et al. (2014), Vidovic and Martill (2014), and Britt et al. (2018). In addition, four new characters (#90, 110, 132, 135) were developed for this study.

This new dataset was analyzed in command-line TNT v. 1.6 (Goloboff & Catalano, 2016) using the traditional (heuristic) search option with 1000 replications and tree bisection reconnection (TBR) swapping algorithm holding 10 trees per replication (with a maximum of 10,000 trees held). All characters were equally weighted with 21 characters being ordered (4, 5, 6, 23, 26, 38, 40, 73, 85, 94, 102, 105, 111, 112, 114, 115, 116, 117, 118, 130, 134). Following the initial search and generation of a strict consensus tree, the ‘Pruned Trees’ function was implemented (using the command ‘*prunelsen*’) to identify and prune unstable taxa in order to increase resolution in a strict reduced consensus. Bremer support values were calculated using the Bremer.run script available at http://phylo.wikidot.com/tntwiki#TNT_scripts (accessed: October 26, 2021). Bootstrap values were calculated using the command ‘resample replications 1000 boot’. Additional details of the analysis are provided in the Supplementary Material S1, section 3.

Institutional Abbreviations—**BSPG**, Bayerische Staatssammlung für Paläontologie und Geologie, Munich, Germany (formerly **BSP**); **CYCB**, Chaoyang Geological Park, Chaoyang City, Liaoning Province, China; **HGM** Henan Geological Museum, Zhengzhou, Henan Province, China; **IVPP**, Institute of Vertebrate Paleontology and Paleoanthropology, Beijing, China; **JPM**, Jehol Paleontological Museum, Chengde, Hebei Province, China; **NHMUK**, Natural History Museum, London, U.K.; **PMOL**, Palaeontological Museum of Liaoning, Shenyang Normal University, Shenyang, China; **STM**, Shandong Tianyu Museum of Nature, Linyi, Shandong Province, China; **ZMNH**, Zhejiang Museum of Natural History, Hangzhou, China.

SYSTEMATIC PALEONTOLOGY

PTEROSAURIA Kaup, 1834

MONOFENESTRATA Lü, Unwin, Jin, Liu, Ji, 2010

DARWINOPTERA Andres, Clark, Xu, 2014

Ceoptera evansae, gen. et sp. nov.

(Figs. 1, 2, 3, 4, 5, 6, 7, 8 and 9, Supplementary Material 1, Figs. S2, S3, S4, S5, S6 and S7)

Holotype—NHMUK PV R37110, an associated partial skeleton in three contiguous blocks consisting of: seven vertebrae (four dorsals, one caudal, and two that are too poorly preserved to identify with certainty); fragments of the sternum and pelvis; a complete scapulocoracoid; and multiple elements of the forelimb (including wrist bones and a complete wing-metacarpal) and hind limb (Figs. 1–9) (see Supplementary Information S1,

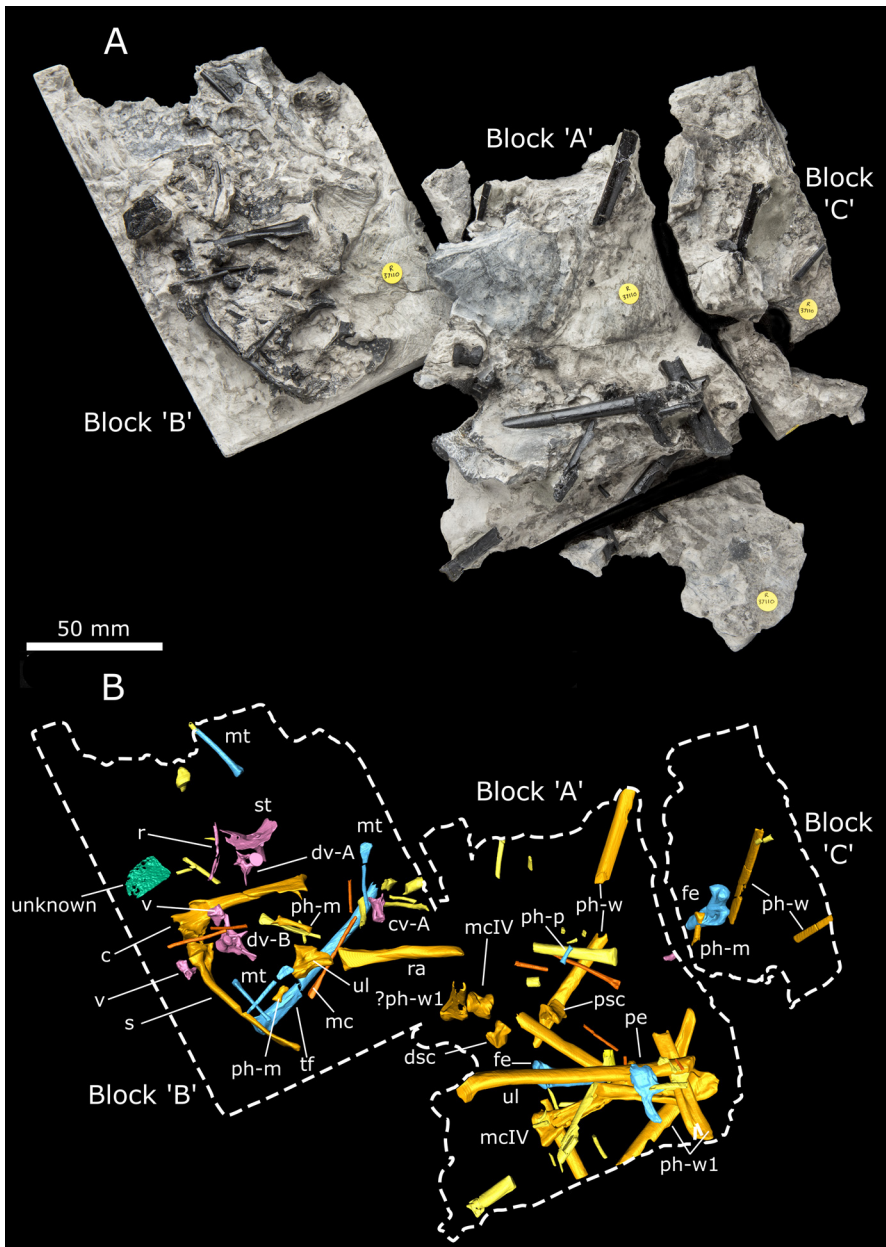


FIGURE 1. NHMUK PV R37110, the holotype of *Ceoptera evansae*, approximately as it was found (top) and by CT reconstruction with elements (bottom). Letters indicate the blocks as discussed in the text. **Abbreviations:** c, coracoid; cv, caudal vertebra; dsc, distal syncarpal; dv, dorsal vertebra; fe, femur; m, manual-phalanx; mc, metacarpal; mt, metatarsal; p, pedal-phalanx; pe, pelvis; ph, phalanx; psc, proximal syncarpal; r, rib; ra, radius; s, scapula; st, sternum; tf, tibia + fibula; ul, ulna; v, vertebra; w, wing-phalanx.

sections 4–5 for additional images, lists of preserved material and measurements).

Type Locality and Horizon—Cladach a’Ghlinne, north of Elgol, Isle of Skye, Scotland, U.K.; Kilmaluag Formation (Bathonian, Middle Jurassic) (Barrett, 2006; Evans et al., 2006; Panciroli et al., 2020).

Etymology—The generic name is composed of the Scottish Gaelic word *cheò* or *ceò* (pronounced ‘ki-yo’), meaning mist (in reference to the common Gaelic name for the Isle of Skye *Eilean a’ Cheò*, or Isle of Mist), and the Latin *ptera*, meaning wing (feminine). The specific epithet honors Prof. Susan E. Evans for her many years of anatomical and paleontological research, in particular on Skye, and in introducing us to this locality, thereby making this find possible.

Diagnosis—*Ceoptera* is distinguished from all other pterosaurs by two features: (1) the presence on the distal (sternal) portion of the coracoid shaft of a well-developed, elongate, narrow, sub-rectangular bony flange (probably a site for insertion of the

m. sternocoracoideus) with an irregular ‘wavy’ free margin, which extends proximally for almost one-quarter of the length of the coracoid; and (2) the lateral surface of the posterior, dorsally expanded, portion of the post-acetabular process of the ilium bears a prominent depression divided in two by a low rounded vertical ridge.

DESCRIPTION

A detailed anatomical map of the elements currently identified for *Ceoptera evansae* and skeletal drawing (Fig. 10) indicates the presence, completeness, and preservation of skeletal elements in NHMUK PV R37110.

As the specimen was subdivided into several blocks during collection and preparation, the description, below, lists the elements found in each block, in order to demonstrate the location of each element within the block and relative to each other. Elements are

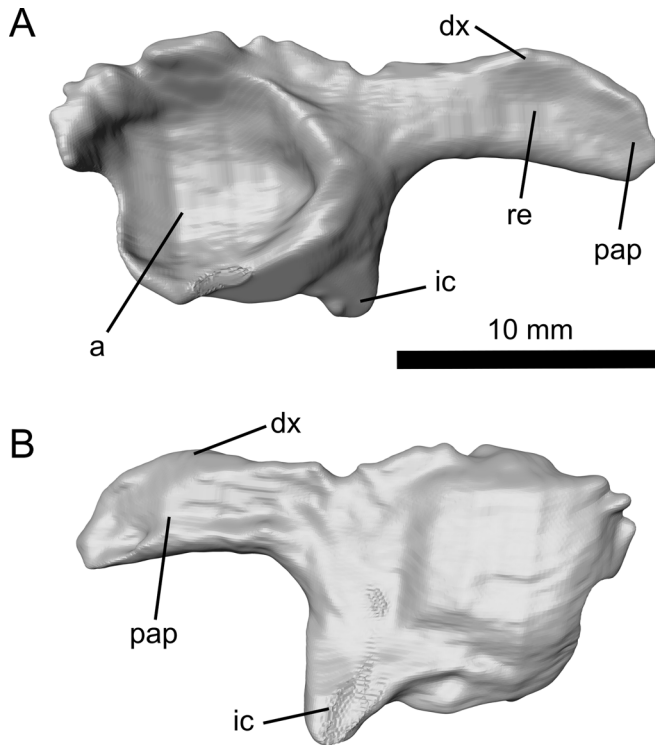


FIGURE 2. Reconstruction of the acetabulum and postacetabular process of the left pelvis of *Ceoptera evansae* (NHMUK PV R37110), in **A**, lateral, and **B**, medial views. **Abbreviations:** **a**, acetabulum; **dx**, dorsal expansion; **ic**, ischium; **pap**, postacetabular process; **re**, recess.

mostly disarticulated but closely associated and many remain partially embedded, or fully enclosed, within the matrix. In these cases, CT-scanning was used to identify and visualize individual elements. Measurements for the better-preserved elements are listed in Supplementary Material 1, section 5, Table S1.

Block A

The elements found in Block A can be viewed in Figures 1–5 and S2 and are described in detail below.

Pelvis (L)—As preserved, this consists of a complete postacetabular process of the ilium and portions of the ischium and ilium that bear the acetabulum (Fig. 2). The latter is subcircular and relatively deep, with well-developed dorsal, posterior, and posteroventral margins. The postacetabular process of the ilium extends posteriorly, and the ventral profile, which is almost straight, is oriented at right angles to the posterior margin of the ischium. The process is elongate but relatively robustly constructed (maximum depth = 37% of length in lateral view). The base of the process is slightly constricted, while the crescent-shaped posterior portion is gently expanded dorsally. Unusually, almost the entire lateral surface of the posterior portion of the process appears to be recessed. The margins of this recess are bounded by a ridge of bone that defines the outer rim of the process, and the recess itself is divided in two by a low, rounded, vertical ridge, resulting in anterior and posterior sub-recesses of approximately equal size.

In almost all pterosaurs where the morphology of the postacetabular process of the ilium is determinable, the lateral surface of this structure is either flat, or slightly convex. In non-monofenestrans the post-acetabular process of the ilium is elongate, slender, lacks any dorsoventral expansion, and is usually directed caudally, although in some cases, e.g.,

Dimorphodon (Sangster, 2021) and *Campylognathoides* (Padian, 2008), the basal portion may be angled posterodorsally, while the distal portion is directed posteriorly. In addition, the process usually tapers distally, although in a few cases, such as *Dimorphodon* (Sangster, 2021) and *Rhamphorhynchus* (Wellnhofer, 1975), the distal terminus may bear a slightly bulbous expansion. A few relatively basally branching pterodactyls, e.g., *Altmuehlopterus rhamphastinus*, retain (presumably) the morphology observed in non-monofenestrans, otherwise, however, monofenestrans are distinguished by a post-acetabular process that is dorsally expanded, although the shape and extent of this expansion varies within Monofenestrata.

In terms of its general morphology, proportions, and orientation the fragmentary left pelvis preserved in *Ceoptera* is identical to that of darwinopterans including *Darwinopterus* (Lü et al., 2011—HGM 41HIII-0309A; Wang et al., 2010—IVPP 16049), *Changchengopterus* (Zhou & Schoch, 2011—PMOL AP-00010), *Kunpengopterus* (Cheng et al., 2017—IVPP V 23674), and ‘*Archaeoistiodactylus*’ (= *Darwinopterus*) (Lü & Fuchs, 2010—JPM04-0008). Comparison with a range of early-branching forms and pterodactyls suggests that the morphology of the postacetabular process of the ilium of darwinopterans and *Ceoptera* is unlike that of other pterosaurs and may be unique to Darwinoptera.

Ulna (R)—This element, exposed on the surface of block A, is largely uncrushed, and has a partially preserved proximal articulation but lacks its distal termination (Fig. 3). The proximal condylar region is medially inflected, exhibits a well-developed ventral expansion, and bears two distinct, subcircular, slightly dished articular facets separated by a low ridge. Immediately distal to the proximal expansion the anterodorsal margin of the ulna shaft bears a small, but distinct, proximally directed, flange-like tubercle, presumably a muscle attachment site. The morphology of the ulna corresponds to that of darwinopterans such as *Darwinopterus modularis* (ZMNH M8802; Lü et al., 2011; DMU, pers. obs.) but this differs little from that of other Jurassic pterosaurs.

Proximal Syncarpal (R)—The right proximal syncarpal is complete, but preserved entirely within the matrix and was made visible using CT-scanning (Fig. 1). It is located ventral to the medial carpal and closely associated but not articulated with it. This syncarpal is completely fused into a single composite element. Details are difficult to discern but the irregular pentagonal outline, with steeply sloping anterodorsal and posterodorsal margins in proximal or distal view, is comparable to that exhibited by the same element in *Kunpengopterus* (Cheng et al., 2017:fig. 2) and contrasts with the subrectangular profile of the proximal syncarpal in non-monofenestrans, for example *Dimorphodon* (Sangster, 2021:fig. 13e) and *Rhamphorhynchus* (Wellnhofer, 1975:fig. 12), in which the dorsal profile is relatively flat. The distal aspect bears two large grooves separated by an obliquely oriented ridge that trends anteroventral to posterodorsal, as found in monofenestrans and some relatively derived non-monofenestrans such as *Rhamphorhynchus* (Wellnhofer, 1975:fig. 12). This contrasts with basally branching forms such as *Dimorphodon* where the ridge separating the upper and lower groove is oriented horizontally (Sangster, 2021:fig. 13).

Distal Syncarpal (L)—This element is complete but enclosed entirely within matrix (Figs. 1, S2). The syncarpal is blocky in shape, seemingly completely fused, and in terms of its general shape and proportions comparable to the distal syncarpal of other Middle and Late Jurassic pterosaurs, but fine anatomical details are not discernible. In ventral view, as is typical for pterosaurs, the proximal margin, which articulated with the proximal syncarpal, is markedly convex while the distal margin, which articulated with the metacarpus, is flat.

Metacarpal IV (L)—This metacarpal is entirely buried within matrix. The diaphysis is slightly compressed but otherwise this element is complete and well preserved (Figs. 1, 4, S2). The

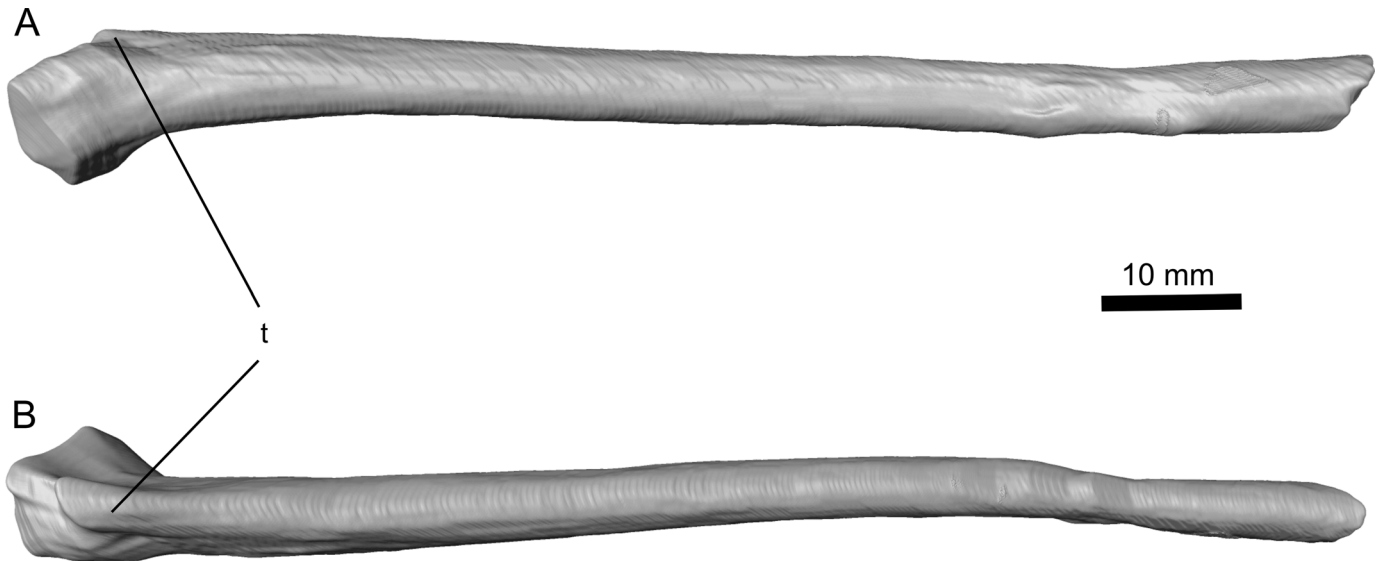


FIGURE 3. The partially preserved right ulna of *Ceoptera evansae* (NHMUK PV R37110), in **A**, ventral, and **B**, dorsal views. **Abbreviations:** t, tubercle.

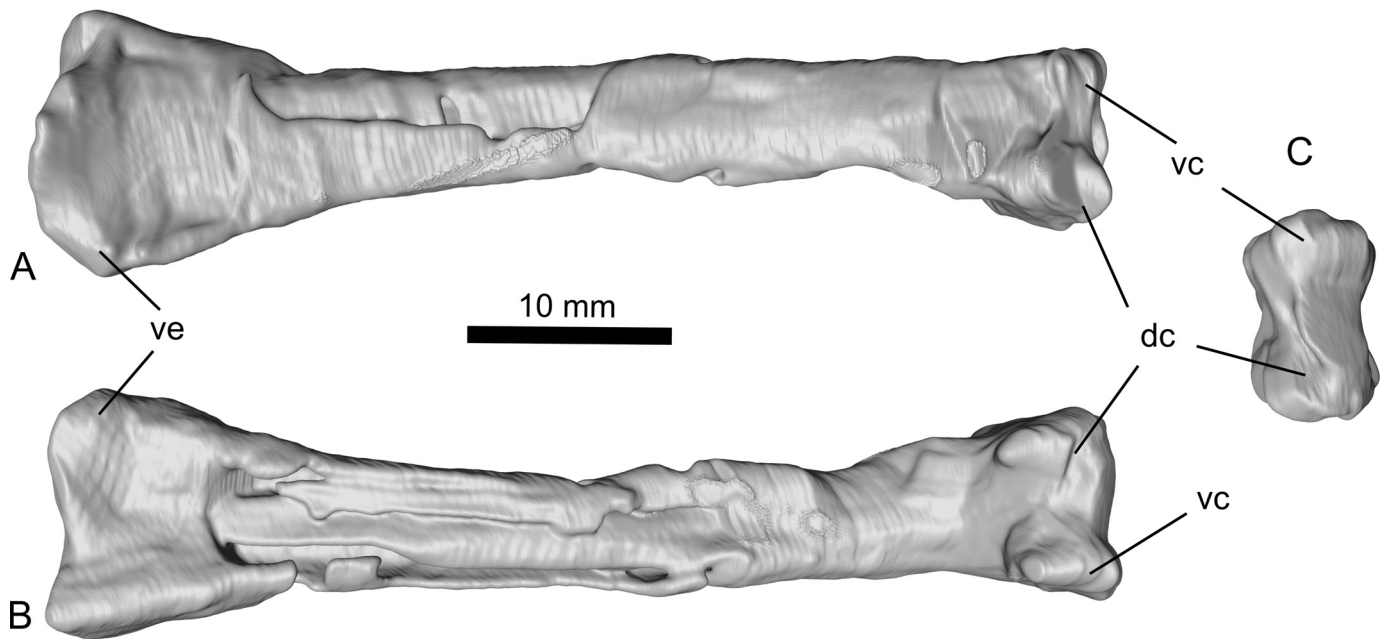


FIGURE 4. Complete left metacarpal IV of *Ceoptera evansae* (NHMUK PV R37110), in **A**, anterior; **B**, posterior; and **C**, distal views. **Abbreviations:** dc, dorsal condyle; vc, ventral condyle; ve, ventral expansion.

wing-metacarpal is robustly constructed and relatively elongate with a length/maximal depth (anterior aspect) ratio (LD) of 3.9. This falls well within values for darwinopterans (LD = 3.5–4.5) and is considerably greater than for any non-monofenestratan pterosaurs, which have a relatively short wing-metacarpal (LD <3.5), and lower than that for any pterodactyloid (LD >4.5), including the basally branching-most forms such as *Rhamphodactylus* (LD = 4.55).

The proximal termination has a prominent ventral expansion and a marked anterior projection at about mid-height on the anterior aspect. The diaphysis is anteroposteriorly compressed, of similar depth throughout much of its length, and lacks a

‘notch’ in the dorsal surface just proximal to the distal ginglymus, which in other pterosaurs accommodates the wing-phalanx when it is fully flexed (Wellnhofer, 1975:fig. 13c). A muscle scar immediately proximal to this ‘notch’ that is usually present in other pterosaurs also appears to be absent.

As is typical for pterosaurs, the distal expansion consists of a double condyle, the dorsal slightly larger than the ventral. In distal view, the ‘hourglass-shaped’ profile of the condyles appears slightly offset as, for example, in *Rhamphorhynchus* (Wellnhofer, 1975:fig. 13c): the dorsal condyle projects further posteriorly than the ventral, while the latter projects further anteriorly than the dorsal condyle. In non-monofenestratans

(e.g., *Dimorphodon*, *Dorygnathus*, and *Rhamphorhynchus*), the dorsal and ventral profiles of the dorsal and ventral condyles, viewed in anterior or posterior aspect, are more or less parallel to each other and to the long axis of the metacarpal shaft (cf. Galton, 1981:fig. 2a–p). By contrast, in *Ceoptera*, the darwinopterans *Wukongopterus* (Wang et al., 2009), *Kunpengopterus* (Cheng et al., 2017), and *Changchengopterus* (Lü, 2009), and the basally branching pterodactyloid ‘*Rhamphodactylus*’ (DMU, pers. obs.) and other more derived pterodactyloids (cf. Galton, 1981:fig. 2p–t; Wellnhofer, 1978:fig. 12), the dorsal and ventral profiles of the dorsal and ventral condyles diverge distally away from the long axis of the metacarpal, such that the condyles have a sloping rather than flat profile in anterior and posterior view. Preservation precludes verification of this feature in many pterosaurs, but it may prove to be another distinctive difference between non-monofenestratan and monofenestratan pterosaurs.

Metacarpal IV (R)—This element lacks the proximal end and much of the diaphysis but is otherwise well preserved (Figs. 1, S2). Its external morphology corresponds in all respects to that described for the left metacarpal IV. The cortical thickness, exposed at the point where the diaphysis is fractured, ranges from 0.93 mm in the narrowest segment of the section up to 1.82 mm in the broadest.

Metacarpals/Metatarsals—Several elongate slender elements likely represent metacarpals that supported the ungual-bearing manus digits, or metatarsals I–IV (Figs. 1, S2). One element that bears a slightly expanded incipiently ‘hourglass-shaped’ profile in proximal view is most likely a metatarsal.

Wing Phalanx (WP) One (L)—This element is represented by the proximal articulation and a short section of the diaphysis (Figs. 1, S2). The proximal articulation, as is typical for pterosaurs, is strongly expanded anteriorly with a rounded profile that gently descends into the diaphysis distally. The posterior expansion is less pronounced and sharply pointed. It fades into the diaphysis at about the same point as the anterior expansion. The proximal articulation supports a double cotyle: the dorsal cotyle takes the form of a gently arcuate shallow groove, that is anteroposteriorly elongate and extends across much of the articulation. The ventral condyle is much shorter and confined to the anterior half of the articulation. The diaphysis has a flattened oval cross section. The anatomy and proportions of the WP1 of *Ceoptera* lack any distinctive features and are typical for many pterosaurs, including darwinopterans.

Wing Phalanx One—This element consists of a distal portion of a WP1, possibly the complementary portion to the proximal end of the left wing phalanx one.

Wing Phalanx Fragments—Block A contains several fragments that, due to their distinctive flattened-oval cross section, are identified as short sections of wing phalanges (Figs. 1, S2). Their breadth is markedly less than that for the diaphysis of wing phalanx one indicating that they likely represent wing phalanx two or three.

Femur (R)—The right femur in block A (Figs. 5, S2) is represented by much of the diaphysis and the distal articulation (Fig. 5C–E). The diaphysis is slightly bowed laterally with a gently convex lateral profile in anterior or posterior aspect and, as in other pterosaurs, is subcircular in cross section. The distal articulation consists of two condyles, the medial slightly more robustly constructed than the lateral, and separated from each other by a shallow sulcus. Comparable morphology is found in many other pterosaurs, including darwinopterans.

Pedal Phalanx—A small, slender, relatively elongate bone is likely a pedal phalanx (Fig. 1) rather than a manual phalanx as the latter tend to be more robustly constructed. The proximal articulation is gently expanded and bears a shallow cotyle, whose width is somewhat greater than its height. The distal articulation is also gently expanded and roller-shaped: highly

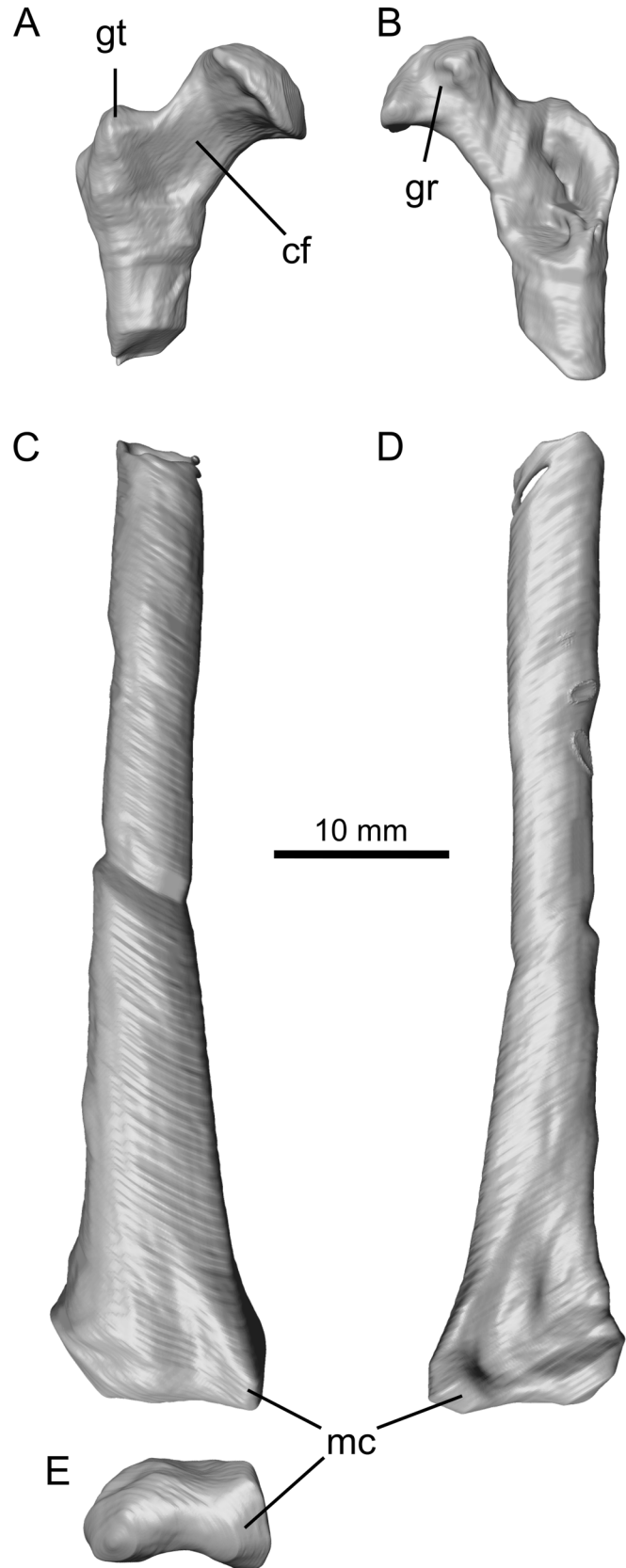


FIGURE 5. Right femur of *Ceoptera evansae* (NHMUK PV R37110), lacking a short section of the diaphysis, in **A**, **C**, anterior, **B**, **D**, posterior, and **E**, distal views. The proximal portion (**A**, **B**) is located in Block C while the distal portion (**C**–**E**) is located in Block B. **Abbreviations:** **cf**, collum femoralis; **gr**, groove; **gt**, greater trochanter; **mc**, medial condyle.

convex along the dorsoventral axis and slightly concave mediolaterally.

Block B

The elements found in Block B can be viewed in [Figures 1, 6–9](#) and S3–5 and are described in detail below.

Sternum—The sternum is completely enclosed within the matrix and lacks most of the thin posterior margins of the sternal plate but retains much of its 3D shape ([Figs. 1, 6, S3](#)). The cristospine is short, deep, robustly constructed, and bears a pair of crescentic coracoid facets, the right located immediately ventral to the left. The dorsal surface of the sternum is pierced by a small pneumatic opening at the junction of the cristospine and the sternal plate. The anterior margins of the sternal plate are thickened and directed latero-dorsally at about 40° above the horizontal such that, when viewed in anterior aspect, the sternal plate presents a shallow ‘V’-shaped profile.

Among pterosaurs a short, deep, relatively broad-based cristospine, comparable to that present in NHMUK PV R37110, seems to be restricted to darwinopterans and is observed, for example, in *Darwinopterus* (e.g., Lü et al., 2010, 2011; Wang et al., 2010), *Kunpengopterus* (Wang et al., 2010), and, seemingly, in *Changchengopterus* (Zhou & Schoch, 2011). The sternal cristospine of *Fenghuangopterus* also appears to be broad-based (Lü et al., 2010), but the cristospine is relatively more elongate than in darwinopterans and its apparent robustness may be partly due to crushing. In ‘*Rhamphodactylus*’ (BSPG 2011 I 133) the outline of the cristospine is closely comparable to that of *Ceoptera*, but the sternal plate is subcircular rather than trapezoidal as in darwinopterans.

Rib—A single, incomplete, poorly preserved early rib is present, lacking the distal termination ([Figs. 1, S3](#)).

Dorsal Vertebra (DV) A—A well-preserved, near complete, and largely three-dimensionally preserved dorsal vertebra ([Figs. 1, 7A, B, S3](#)). The relatively small size of this dorsal vertebra, the slenderness of the transverse processes, and the low neural spine indicate a position toward the posterior end of the dorsal series. As for dorsal vertebra B the base of the transverse process is relatively broad extending forward to buttress the prezygapophysis.

Dorsal Vertebra B—Located between the scapula and coracoid this is the best-preserved, most complete, and largest of the four dorsal vertebrae present in NHMUK PV R37110 ([Figs. 1, 7C, D, S3](#)). The morphology of this dorsal vertebra, and the others described below, corresponds in general to that of other pterosaurs but also exhibits subtle but distinctive features. The centrum is strongly waisted with a typical spool-shaped profile, the transverse processes are robust and well developed, and the neural spine is relatively tall. These features suggest that this vertebra occupied a relatively anterior position within the dorsal series. This is consistent with the location of the capitular facet, which extends to about half the length of the transverse process, a configuration that, in other pterosaurs including *Darwinopterus* (DMU, pers. obs.) corresponds to dorsal vertebra #5 or #6 (e.g., Wellnhofer, 1975).

The transverse processes are directed laterally and slightly above the horizontal (seen in anterior or posterior aspect) and seem to be strengthened by a narrow ridge that extends from the base of the neural process almost to the distal termination of the transverse process. The dorsal profile of the transverse process is rather unusual: the base of the buttress supporting the capitular facet extends anteriorly, supporting the lateral margin of the prezygapophysis. In addition, the same buttress, taking the form of a short flange, extends a little distal to the capitular facet. These features appear to be absent in other

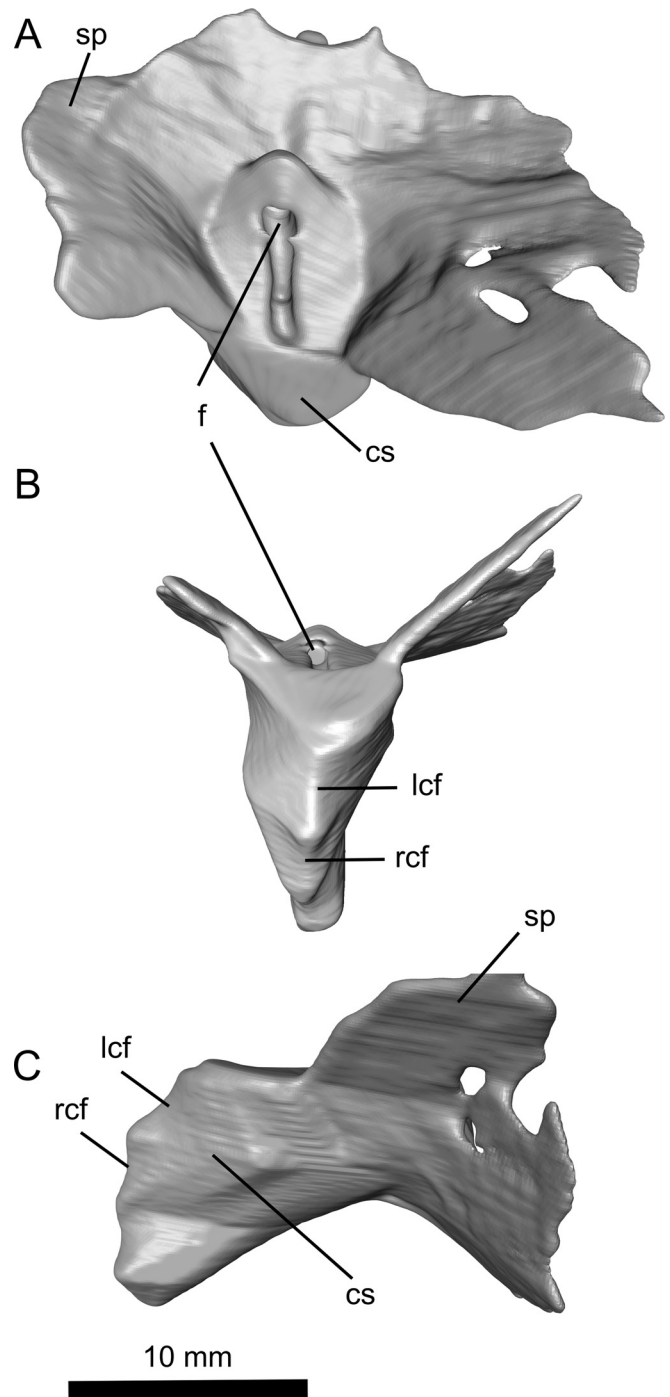


FIGURE 6. Reconstruction of the sternum (primarily the cristospine) of *Ceoptera evansae* (NHMUK PV R37110), in **A**, dorsal, **B**, ventral, and **C**, left lateral views made from CT scans. **Abbreviations:** **cs**, cristospine; **f**, foramen; **lcf**, left coracoid facet; **rcf**, right coracoid facet; **sp**, sternal plate.

pterosaurs such as *Rhamphorhynchus* (Wellnhofer, 1975) and *Pterodactylus* (DMU, pers. obs.), but are present in *Darwinopterus* (ZMNH M8782).

The neural arch and centrum appear to be fully fused as seems to be the case for all other vertebrae of NHMUK PV R37110 in which this condition can be assessed.

Dorsal Vertebra C—This vertebra is fully enclosed within the matrix and only visible in high-resolution scans ([Figs. S4, S5](#)). In ventral view the centrum is prominently waisted.

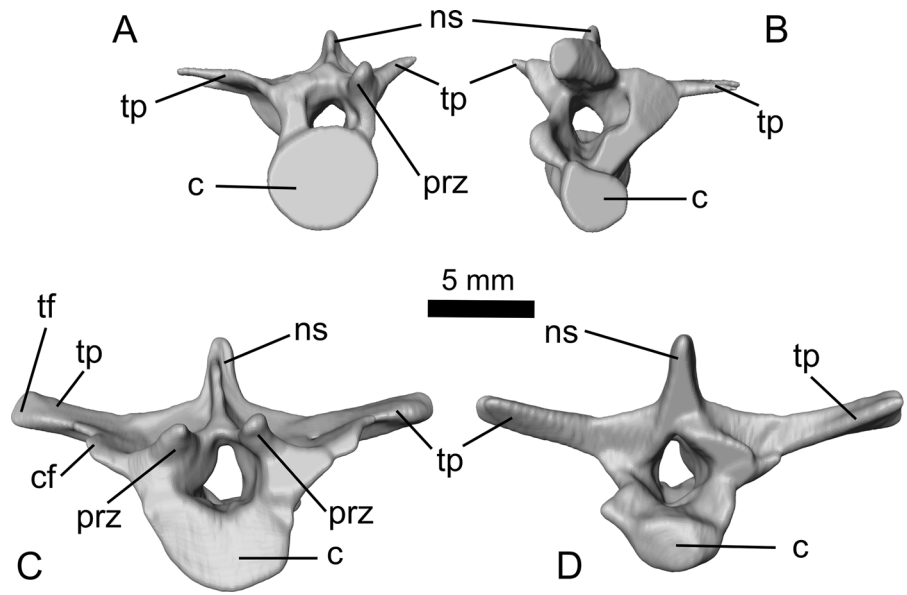


FIGURE 7. Dorsal vertebrae A (A, B) and B (C, D) of *Ceoptera evansae* (NHMUK PV R37110), in A, C, anterior and B, D, posterior views. **Abbreviations:** c, centrum; cf, capitular facet; ns, neural spine; prz, prezygopophysis; tf, tubercular facet; tp, transverse process.

Dorsal Vertebra D—This well-preserved dorsal vertebra is fully enclosed within the matrix and only visible in high resolution scans (Figs. S4, S5).

Caudal Vertebra A—This small, lightly built, relatively elongate vertebra (Figs. 1, S3–S5), lacking transverse processes and with a low, subtriangular neural spine, represents an anterior caudal corresponding, in darwinopterans such as *Darwinopterus* (HGM HIII-0309A), to caudal #6 or #7. The development of attenuate anterior and posteriorly directed processes on the dorsal surfaces of, respectively, the pre- and postzygapophyses hints at the presence of elongate filiform processes in the tail of *Ceoptera*.

Other Vertebrae (A, B)—Two poorly preserved ?dorsal vertebrae (Figs. 1, S4), one consisting of part of the centrum and the neural arch, and the other a partial centrum, respectively, are also present but do not provide any further anatomical information.

Scapulocoracoid (R)—The right scapula and coracoid are complete and exposed on the surface of block B (Figs. 1, 8, S3–S5). They are preserved adjacent to each other and, based on the shape of the joint surfaces, were unfused rather than separated by breakage. The glenoid is positioned primarily on the scapula and to a lesser extent by the coracoid ventrally. The scapula is elongate, strap-like, and gently bowed laterally, when viewed in anterior aspect, and bears a distinctive slightly bulbous distal termination capped by a smooth, possibly articular, facet oriented obliquely to the long axis of the scapula shaft.

The coracoid is markedly expanded proximally with a well-developed anteriorly directed acrocoracoid, as in other darwinopterans (Fig. 8). Unlike other non-pterodactyloids, except for darwinopterans, the coracoid bears a prominent sub-triangular brachial flange on its lateral surface. The diaphysis has a rounded triangular cross section. Its distal portion, the terminus of which articulated with the sternum, is strongly expanded, especially along its dorsal margin, which bears a narrow, elongate flange with a ‘wavy’ free margin, that is interpreted here as an insertion site for the m. sternocoracoideus.

Compared with non-monofenestratans the scapulocoracoid is relatively derived, with a scapula that is markedly longer than the coracoid. In darwinopterans, as in most other pterosaurs, the distal (sternal) end of the coracoid is markedly expanded.

The expanded bulbous distal termination of the scapula is a highly unusual feature and typical of darwinopterans. In *Darwinopterus* (Lü et al., 2011—ZMNH M8802; Wang et al., 2010—IVPP V16049), *Kunpengopterus* (Cheng et al., 2017; IVPP V23674), and *Wukongopterus* (Wang et al., 2009; IVPP V15113) the scapula is nearly identical in morphology to that of *Ceoptera*. Moreover, in ZMNH M8802 the proximal surface of the distal expansion also appears to bear an articular facet. The distal end of the scapula is also expanded in *Changchengopterus* (Lü, 2009; basally branching monofenestratan *Douzhanopterus* (Wang et al., 2017; STM 19-35). Whether the scapula articulated with the vertebral column in *Ceoptera* and other darwinopterans is not yet known.

Radius (L)—The radius preserves the proximal articulation and much of the diaphysis, which is cylindrical in shape, but lacks the distal termination (Figs. 1, S3). The proximal articulation consists of a simple, rounded, slightly dished facet, as in other pterosaurs.

Ulna (L)—An incomplete limb bone, adjacent to the radius, may be the poorly preserved remains of the left ulna (Figs. 1, S3).

?Wing Phalanx One (R)—Adjacent to the previous two elements, a limb bone with a strongly expanded (?) proximal end appears to represent the incompletely preserved remains of the proximal end of the right wing phalanx one (Figs. 1, S3). Notably, the proximal extensor tendon tubercle appears to be absent and presumably was not fused to the wing phalanx.

Metacarpal—Adjacent to the distal end of the radius an elongate, slender element is present (Figs. 1, S3). It has a markedly expanded termination bearing a well-developed condyle that is triangular in terminal view, and likely represents a metacarpal that articulated with one of the claw-bearing digits of the manus.

Manual Phalanx (Penultimate)—A small, simple, slightly elongated element medial to the scapula, with a flattish proximal articular facet and bicondylar distal condyles, likely represents an intermediate phalanx from one of the three claw-bearing digits of the manus (Fig. 1).

Pelvis (R)—The preserved part of the right pelvis consists of the postacetabular process of the ilium, a slender portion of the posterior margin of the ischium, and the posterodorsal rim of the acetabulum (Figs. S4, S5). This fragment corresponds

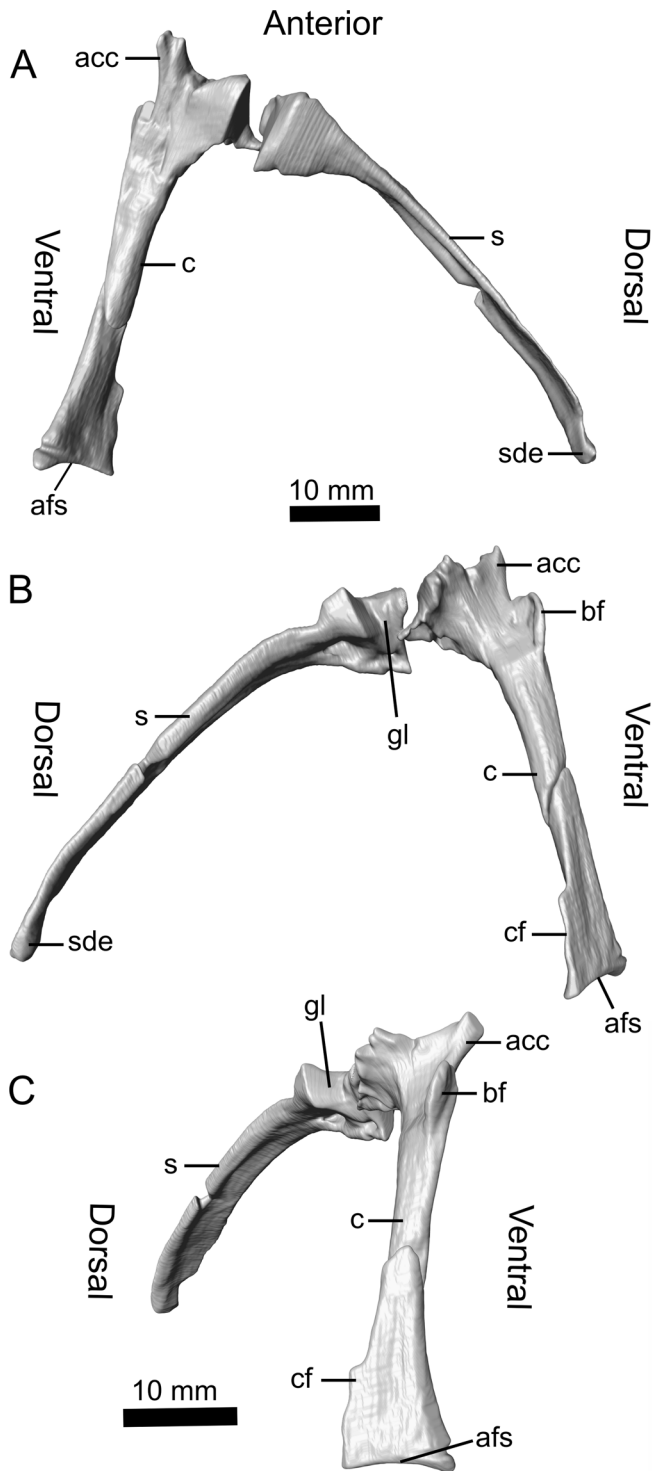


FIGURE 8. Reconstruction of the right scapulocoracoid of *Ceoptera evansae* (NHMUK PV R37110), made from CT scans in **A**, lateral and **B**, medial views. **C**, reveals a close-up of the expanded sub-triangular brachial flange of the coracoid, one of the diagnostic characters of this taxon. **Abbreviations:** acc, acrocoracoid process; afs, articular facet for sternum; bf, brachial flange; c, coracoid; cf, coracoid flange; gl, glenoid; s, scapula; sde, distal expansion of scapula. The top scale bar is for **A** and **B**.

closely, in terms of the portion of the pelvis preserved and its morphology, to the fragmentary left pelvis (see above), but is not as well preserved as the latter. This element is only visible

in the high-resolution scans of block B and is preserved entirely within the matrix.

Tibia and Fibula (?L)—The proximal articulations of a fused left tibia and fibula, exposed in anterior view, together with short sections of their co-ossified diaphyses, are preserved on the surface of block B (Figs. 1, 9, S3–S5). The combined proximal (articular) surface is slightly dished transversely. In anterior aspect the proximal profile of the tibia-fibula is flat and perpendicular to the long axis of the element. The proximal termination of the tibia projects slightly medially then curves rapidly into the shaft of the tibia. The lateral apex of the fibula is more rounded and the shaft, which is closely appressed to the tibia with no interosseous space, is relatively robust and more than one-half the width of the tibia shaft. The preserved portion of the tibia-fibula of *Ceoptera* corresponds closely in all anatomical details to those of other darwinopterans, including *Darwinopterus* (Lü et al., 2011; HGM 41HIII-0309A), *Changchengopterus* (Zhou & Schoch, 2011; PMOL AP-00010), and *Wukongopterus* (Wang et al., 2009; IVPP V15113).

Metatarsals—Several incomplete, long, slender elements that are markedly thinner than the metacarpal described above likely represent the remains of metatarsals I–IV (Figs. 1, S3–S5).

Pedal Ungual—An isolated pedal unguis, preserved on the underside of block B (Fig. S3), is well preserved, lacking only its distal tip. The unguis is elongate (length = 3.6 × width) and gently recurved. The flexor tubercle is elongate, extending about 40% the total length of the unguis and has a distinctive geometric rather than rounded profile, with a flat ventral margin, anterior to which its profile slopes gently into the main body of the claw. The posterior margin of the tubercle is angled at about 45° to the ventral margin. The articular facet is only slightly dished. Within Pterosauria, this particular unguis morphology is largely restricted to darwinopterans, including *Darwinopterus* (Lü et al., 2011; HGM 41HIII-0309A, IVPP V16049), *Kunpengopterus* (IVPP V16047), *Changchengopterus* (Zhou & Schoch 2011; PMOL AP-00010), and *Wukongopterus* (Wang et al., 2009; IVPP V15113). Some pedal unguis of *Pterodactylus* and *Germanodactylus* appear similar but lack the elongation of the unguis tip.

Unidentified/Non-pterosaurian Bone—The surface of block B bears a subquadratic bone of uncertain identity (Figs. 1, S3). It does not compare well with any element from the pterosaur skeleton and exhibits a rough, porous texture. It is possibly a crocodylian osteoderm or a fragment of turtle plastron or carapace.

Block C

Caudal Vertebra—Remains of a small caudal vertebra are preserved adjacent to the femur (Figs. 1, S6).

Femur (R)—Block C preserves the proximal portion of the right femur (Figs. 1, 5A, B, S6). The femur has a gently convex subcircular caput, bisected in its posteromedial quadrant by a large groove that notches into the terminal profile of the caput. The collum femoris is markedly constricted and the lateral ‘shoulder’ of the femur bears a well-developed greater trochanter. The latter, seen in anterior aspect, projects dorsally above the general profile of the collum femoris where it merges into the diaphysis. This feature is absent in basally branching pterosaurs, but present in darwinopterans and more derived pterosaurs. The collum femoris and caput are directed at approximately 126° to the long axis of the shaft.

Within Darwinoptera, for all taxa where this element is preserved including *Darwinopterus* (Wang et al., 2010) and *Kunpengopterus* (Wang et al., 2010), the morphology of the proximal half of the femur is invariable and compares closely to the femur of *Ceoptera*. There are some minor differences: most notably, in *Ceoptera*, the collum femoris is relatively elongate and seemingly

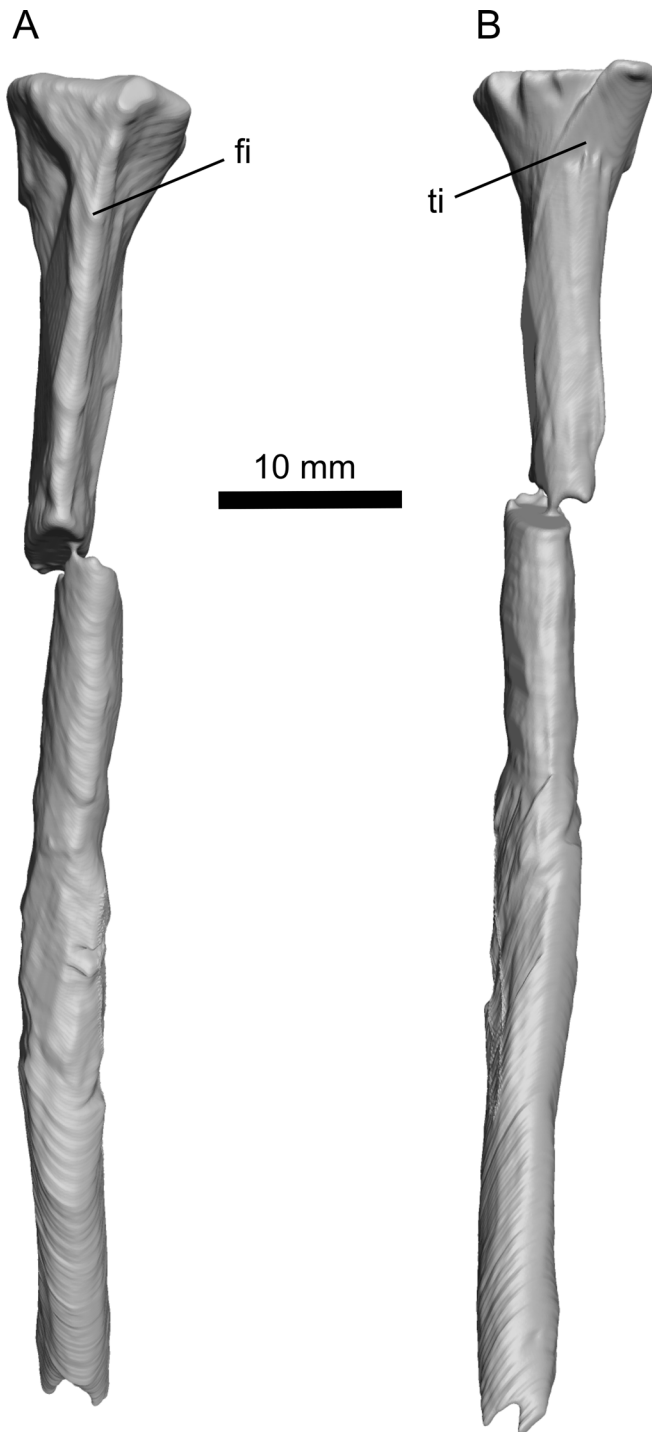


FIGURE 9. Tibia-fibula of *Ceoptera evansae* (NHMUK PV R37110), in A, lateral, and B, medial views. **Abbreviations:** fi, fibula; ti, tibia.

more constricted than in other darwinopterans, in which it appears to be relatively shorter and stouter.

Manual Phalanx—A small, elongate, markedly curved phalanx, likely from one of the manual digits, is located adjacent to the femur (Figs. 1, S6).

Wing Phalanx Fragments—Two fragments, consisting of elongate, somewhat flattened, lath-like diaphyses, lacking articular ends, likely represent portions of the third or fourth wing finger phalanges (Figs. 1, S6).

Isolated Material

Coracoid (L)—The well-preserved distal portion of the left coracoid (Fig. S7) has been isolated from the matrix. This fragment is less complete than the corresponding part of the right coracoid, but insofar as comparisons can be made the two are identical.

Size and Ontogenetic Status

The wingspan of NHMUK PV R37110 was calculated by regressing forelimb length (humerus + ulna + wing-metacarpal + wing-finger) against wing metacarpal length for the following darwinopterans (*Darwinopterus*, *Changchengopterus*, *Kunpengopterus*, and *Wukongopterus*). An estimate of forelimb length for *Ceoptera* was generated using the length of the wing metacarpal and the regression equation. The estimated forelimb length (0.76 m) was multiplied by a factor of 2.1 to generate an estimated wingspan of 1.6 m.

Several compound skeletal structures including vertebrae, the pelvic plates, syncarpals, and the tibia-fibula are fully fused. This, and the presence of bone surfaces with a smooth, dense texture (Bennett, 1993; Dalla Vecchia, 2018), seems to indicate that the holotype of *Ceoptera* was osteologically mature at time of death. By contrast, the absence of fusion of the scapulocoracoid and of the proximal extensor tendon to the wing-phalanx are not consistent with full osteological maturity. Patterns of fusion in the pterosaur skeleton are highly variable, however (e.g., Bennett, 1993; Dalla Vecchia, 2018), and rarely, if ever, follow a strict sequence, even within species. Critically, the presence of multiple examples of fused compound structures suggests that in the case of NHMUK PV R37110 the main growth phase had been completed, and it is doubtful that there would have been any further significant increases in the size of this individual. Ultimately, osteohistological data may provide a more precise understanding of the ontogenetic status of NHMUK PV R37110.

Phylogenetic Analysis

Phylogenetic analysis recovered 2890 most parsimonious trees (MPTs), from which a strict consensus tree was calculated (Supplementary Material S1, section 6, Figs. S8, S9). This contains a monophyletic Darwinoptera that includes *Ceoptera evansae*, several Tiaojishan Formation pterosaurs (*Darwinopterus*, *Wukongopterus*, *Kunpengopterus*, *Changchengopterus*), and *Kryptodrakon*, *Cuspicephalus*, and *Allkaruen* from the Upper Jurassic of China, the U.K., and Argentina, respectively, whose referral significantly expands the content of this clade compared with previous studies (see Supplementary Material S1, section 7 for discussion on the definition of Darwinoptera). Resolution was poor in the region of the tree close to *Ceoptera*, but a posteriori pruning of four unstable taxa, *Cacibupteryx*, *Campylognathoides*, *Douzhanopterus*, and *Haopterus*, produced a reduced strict consensus tree with better resolution (Figs. 11, S10). However, support values for Darwinoptera (and many other clades) are moderate to low (Figs. 11, S9). The list of character changes is available in Supplementary Material S1, section 8a for the strict consensus tree and Supplementary Material S1, section 8b for the strict reduced consensus tree. Note that in the strict consensus tree Darwinoptera is Node 77; in the reduced strict consensus it is Node 79.

Ceoptera exhibits several derived character states that appear to characterize darwinopterans, including an expanded, bulbous distal termination of the scapula (#90.2) and the relative proportions of the wing metacarpal (#110.1) (see Supplementary Material S1, sections 7, 8a, and 8b for further information). *Ceoptera* also exhibits several features (a short, relatively broad cristospine of the sternum; distinctive crescentic shape of

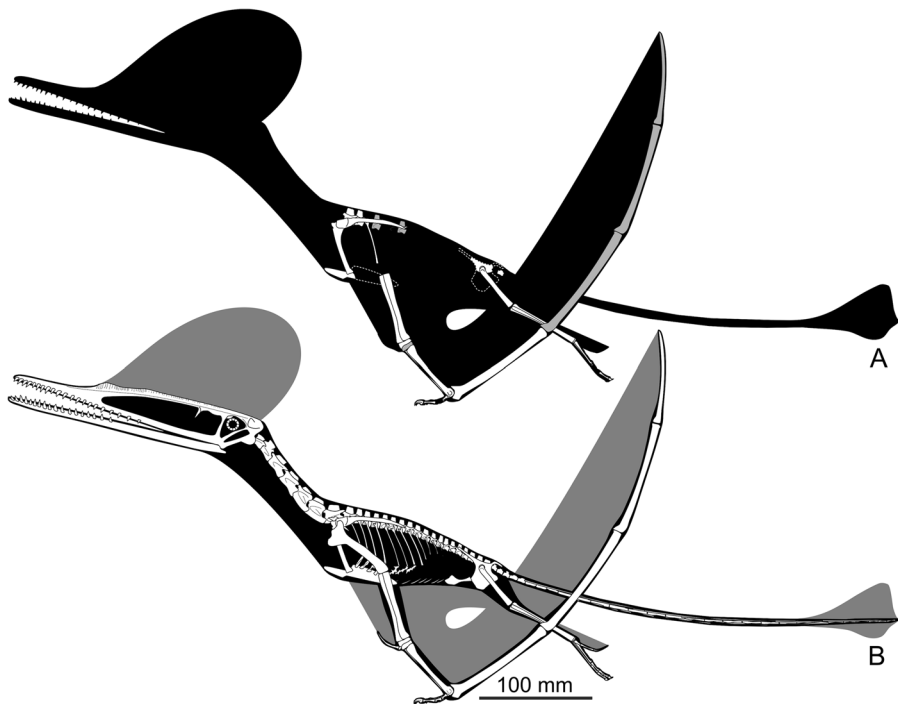


FIGURE 10. Skeletal of *Ceoptera evansae* (NHMUK PV R37110), showing the material that is present (top, with grayed bones indicating partially preserved elements) and an artist's impression of what the entire skeleton would have looked like if complete. Image copyright Mark Witton.

the post-acetabular process of the ilium) that also appear to be restricted to Darwinoptera. Reinforcing the results of the phylogenetic analysis, the skeletal anatomy of *Ceoptera* compares closely to that of typical darwinopterans, such as *Darwinopterus* (Lü, 2009; Lü et al., 2010, 2011).

In the strict consensus tree Darwinoptera and Pterodactyloidea form an unresolved node with *Douzhanopterus* and '*Rhamphodactylus*' (Figs. S8, S9) but in other tree topologies generated by our analysis, as in other studies that include these taxa (Jagielska et al., 2022; Wang et al., 2017; Wei et al., 2021), the latter two resolve as basally branching pterodactyloids, consistent with the presence in these taxa of typical pterodactyloid characters such as the reduction of pedal digit V to a single phalanx (see Supplementary Material S1, sections 8a and 8b for full synapomorphy lists).

DISCUSSION

Ceoptera evansae from the Middle Jurassic of Scotland (Fig. 12) provides important new data on the geographic and stratigraphic range of the controversial clade Darwinoptera, which was thought previously to be a species-poor group restricted largely to the early Upper Jurassic of eastern Asia (Andres et al., 2014; C.-F. Zhou et al., 2017). Critically, new insights into potentially unique anatomical features of darwinopterans, such as the expanded distal termination of the scapula, first identified in *Ceoptera*, contribute new phylogenetic data to the analysis presented herein, which underpins five key findings:

(1) Darwinoptera is Monophyletic

In some previous analyses, the taxa included in this clade formed a paraphyletic cluster of basally branching monofenestratan-grade pterosaurs (Andres et al., 2014; Jagielska et al., 2022; Wang et al., 2017). Pterosaurs such as *Darwinopterus* and *Wukongopterus*, which are represented by relatively complete

skeletons, were united by a uniquely modular anatomy in which the cranium and cervical vertebrae exhibit derived characters typical of pterodactyloids while the remainder of the skeleton appears to be closely comparable to that of early-branching (non-monofenestratan) pterosaurs (Lü et al., 2010, 2011; Wang et al., 2009, 2010, 2017). The relative incompleteness of other putative darwinopterans, such as *Cuspicephalus* (known only from skull remains: Witton et al., 2015), hindered wider recognition of this complex morphological pattern.

Although support for clade monophyly appears to be low on the basis of Bremer and bootstrap values (Figs. 11, S9), this study identified a suite of characters distributed across the skeleton (cranium, sternum, scapulocoracoid, metacarpus, pelvis, pes) that are either unique to darwinopterans, occur in a unique combination, or arose independently in other clades but have a restricted distribution within Pterosauria (Witton et al., 2015). In the strict consensus tree, monophyly of the clade is supported by 14 shared character state changes, with the low support values due to homoplastic distributions of many of these features, although some of this homoplasy is caused by very limited distributions of these character states in parts of the pterosaur tree distant from Darwinoptera. For example, an unusual construction of the second phalanx of the fifth digits (#135.1) is found only in darwinopterans and *Rhamphorhynchus*. The number of synapomorphies is reduced to seven for the reduced strict consensus, due to differences in taxon inclusion. Contrary to earlier studies (Lü et al., 2010; Wang et al., 2009, 2010, 2017) it appears that darwinopterans can no longer be considered as directly transitional between early-branching pterosaurs and Pterodactyloidea, but rather form a sister group to Pterodactyloidea. Nevertheless, it can be inferred from the results of our phylogenetic analysis, in which Darwinoptera and Pterodactyloidea are sister taxa, that the modularity exhibited by darwinopterans was likely derived from early-branching pterodactyloids providing important, if indirect, insights into the origin of the pterodactyloid bauplan.



FIGURE 12. Life reconstruction of *Ceoptera evansae*. Image copyright Mark Witton.

(2) *Ceoptera* is a New Species of Darwinopterans

Two distinctive features, the morphology of the sternal portion of the coracoid and the morphology of the postacetabular process of the ilium, distinguish *Ceoptera* from other darwinopterans.

In most, but not all pterosaurs the distal, sternal termination of the coracoid is transversely expanded to varying degrees, such that the articular cotyle is supported on each side by a small, rounded, or subtriangular narrow buttress, or flange, of bone that rapidly narrows proximally and fades into the shaft of the coracoid. In most cases where the distal termination is expanded it is asymmetric, the medial buttress being more pronounced than the lateral which, not infrequently, is all but absent (e.g., Dalla Vecchia, 2009:fig. 3; Unwin, 2003; Wellnhofer, 1978).

Darwinopterans are unusual in that the lateral flange is also well developed. In most cases, including *Darwinopterus* (e.g., HGM 41HIII-0309A), this expansion is simple in form resulting in a flange with an elongate triangular profile. *Ceoptera* is distinguished from other darwinopterans by the presence of a well-developed, elongate, narrow, subrectangular bony flange with an irregular ‘wavy’ free margin, that extends proximally for almost one-quarter of the length of the coracoid (Figs. 1, 8). Among darwinopterans *Kunpengopterus* is unusual in that the dorsal flange is also relatively elongate and similar in outline to that of *Ceoptera* (Cheng et al., 2017:fig. 4b), but lacks the ‘wavy’ margin and rather abrupt proximal termination of the flange.

The morphology of the post-acetabular process in *Ceoptera* (Fig. 2) is closely comparable to that observed in darwinopterans, notably *Darwinopterus linglongtaensis* (Wang et al., 2010:fig. 5b) from which it differs only in the absence of a lateral depression, in the latter. A lateral depression is present in *Kunpengopterus* (Cheng et al., 2017:fig. 4) but it is small and located in the anterior part of the expanded caudal portion, just caudal to the

constricted portion of the process and quite unlike the condition observed in *Ceoptera*. Moreover, in *Kunpengopterus* the dorsal expansion of the post-acetabular process is much more pronounced than in *Ceoptera*. In other darwinopterans, such as *Darwinopterus modularis*, *Changchengopterus*, and *Wukongopterus*, the post-acetabular process is relatively slender and elongate (length to maximum depth ratio = 3.0–4.0) unlike that of *Ceoptera* in which it is relatively shorter and more robust (length to maximum depth ratio = 2.5).

Finally, it is worth noting that a pelvis and associated hind limb elements (DFMMh/FV 500) of an indeterminate dsungaripterid from the Upper Jurassic of the Langenberg Quarry, Oker, Germany (Fastnacht, 2005:fig. 3) also bears a post-acetabular process with a pronounced depression on its lateral surface. In this case, however, the depression is tear-shaped and extends for much of the length of the process, rather than being confined to the caudal half.

(3) Darwinoptera is a More Inclusive Clade than Inferred Previously

Our analysis shows that in addition to *Ceoptera*, *Darwinopterus* (Lü et al., 2010), and *Wukongopterus* (Wang et al., 2009), other Tiaojishan Formation pterosaurs such as *Kunpengopterus* (Wang et al., 2010) and *Changchengopterus* (Lü, 2009), as well as *Allkaruen* (Codorniu et al., 2016; Cúneo et al., 2013), *Kryptodrakon* (Andres et al., 2014), and *Cuspicephalus* (Witton et al., 2015), can be assigned to Darwinoptera. Originally identified as the earliest-known pterodactyloid (Andres et al., 2014), reassignment of *Kryptodrakon* to Darwinoptera means that *Liaodactylus* (C.-F. Zhou et al., 2017) is now the earliest record for Pterodactyloidea. Mirroring their taxonomic diversity, which already exceeds that of all other principal Jurassic pterosaur clades, darwinopterans also exhibit considerable morphological

diversity. This is most notable in the cranium (Witton et al., 2015) and suggests that Darwinoptera was composed of several distinct sub-clades, although resolution of the clade's internal relationships remains poor and additional work is required in this area.

(4) Darwinopterans Persisted for at Least 25 Million Years and had a Near Global Distribution throughout this Interval

Re-dating of the oldest known darwinopteran, *Allkaruen*, indicates that Darwinoptera extended from at least the late Early Jurassic (Toarcian: Cúneo et al., 2013) to the Late Jurassic (Kimmeridgian), with *Cuspicephalus* the youngest record for the clade (Witton et al., 2015). The seemingly complete absence of darwinopterans in any of the latest Jurassic (Tithonian) pterosaur-bearing Lagerstätten of western Europe suggests that the clade might not have survived to the end of the Jurassic. Darwinopterans have now been reported from western Gondwana (Codorníu et al., 2016), east (Lü, 2009; Lü et al., 2010, 2011; Wang et al., 2009, 2010, 2017) and west Laurasia (this study) and it seems likely that they had achieved a near worldwide distribution by the Middle Jurassic, if not earlier.

(5) Rewriting the First Half of Pterosaur Evolutionary History

Combining the results of this study with other recent fossil finds (Jagielska et al., 2022; Tischlinger & Frey, 2014; Wei et al., 2021; C.-F. Zhou et al., 2017), more precise dating of pterosaur assemblages, most notably the Tiaojishan Formation (Gao et al., 2019), and new key taxa (e.g. *Allkaruen*: Codorníu et al., 2016; Cúneo et al., 2013), reveals greater complexity in the early history of pterosaurs than previously recognized. Mass extinctions at the end of the Triassic seem to have had relatively little impact on pterosaurs, with most principal clades surviving into the Jurassic (e.g., Butler et al., 2013; Dean et al., 2016). A second radiation appears to have taken place in the Early Jurassic leading to the establishment of several important early-branching pterosaur clades: scaphognathines, rhamphorhynchines, darwinopterans, and a lineage that culminated in pterodactyls. In sharp contrast to the paucity of their fossil record, pterosaurs clearly achieved relatively high levels of taxonomic, morphological and, presumably, ecological diversity in the Middle Jurassic. The Late Jurassic witnessed even higher levels of diversity, as almost all of the Middle Jurassic non-pterodactyl clades seem to have persisted through much of this interval alongside the basal radiation of pterodactyls, and the initial radiation of avialans (Cau, 2018). Expansion into unoccupied ecomorphospace by newly evolving clades, rather than competitive displacement, would seem to offer a possible explanation for the co-occurrence, over a period of at least 15 million years, of these diverse groups of Late Jurassic fliers, although quantitative examination of pterosaur and avialian morphospace occupation will be required to test this hypothesis.

DISCLOSURE STATEMENT

No potential conflict of interest was reported by the author(s).

ACKNOWLEDGMENTS

We thank Susan E. Evans for introducing PMB to the locality, J. Anquetin, S. Feerick, and S. Moore-Fay for their participation in the 2006 fieldtrip to Skye and assistance in collecting the specimens, and Scottish Nature and the John Muir Trust for permissions and access to the locality. The Natural History Museum, London and the Palaeontographical Society provided funding. We thank M. Day for access to the specimen, T. Davies for CT-scanning, D. Sykes for an early exploratory

scan, R. Maclean for Gaelic advice, S. Ludwig for access to her pterosaur ungual dataset, and D. Martill, M. O'Sullivan, R. Smyth, and M. Witton for discussions. M. Witton is also thanked for the skeletal and life reconstructions of *Ceoptera* shown in Figures 10 and 12. We thank D. Foffa for assistance with figures. Finally, we thank D. Hone, one anonymous reviewer, the Associate Editor, and the Phylogenetics Editor for their comments, which helped to improve this manuscript.

AUTHOR CONTRIBUTIONS

EMS and PMB designed the project. EMS, DMU, LAJ, and ARC gathered the data. EMS, PMB, DMU, and EEB analyzed the data. All authors contributed to writing and editing the manuscript.

SUPPLEMENTARY FILES

Martin-Silverstone et al SOM 1.doc – additional text and figures

Martin-Silverstone et al SOM 2.nex – nexus file

Martin-Silverstone et al SOM 3.tnt – TNT file

Martin-Silverstone et al SOM 4.tre – Tree file

ORCID

Elizabeth Martin-Silverstone  <http://orcid.org/0000-0003-0139-2109>

David M. Unwin  <http://orcid.org/0000-0002-9312-2642>

Andrew R. Cuff  <http://orcid.org/0000-0001-9509-4297>

Emily E. Brown  <http://orcid.org/0000-0003-3491-5586>

Lu Allington-Jones  <http://orcid.org/0000-0002-7890-0207>

Paul M. Barrett  <http://orcid.org/0000-0003-0412-3000>

LITERATURE CITED

- Andres, B., Clark, J., & Xu, X. (2014). The earliest pterodactyl and the origin of the group. *Current Biology*, 24, 1011–1016.
- Andrews, J. E. (1985). The sedimentary facies of a late Bathonian regressive episode: the Kilmaluag and Skudiburgh Formations of the Great Estuarine Group, Inner Hebrides, Scotland. *Journal of the Geological Society of London*, 142, 1119–1137.
- Bakurina, N. N. & Unwin, D. M. (1995). A survey of pterosaurs from the Jurassic and Cretaceous of the former Soviet Union and Mongolia. *Historical Biology*, 10(3), 197–245. <http://doi.org/10.1080/10292389509380522>
- Baron, M. G. (2020). Testing pterosaur ingroup relationships through broader sampling of avemetatarsalian taxa and characters and a range of phylogenetic analysis techniques. *PeerJ*, 8, e9604. <https://doi.org/10.7717/PEERJ.9604/SUPP-2>
- Barrett, P. M. (2006). A sauropod dinosaur tooth from the Middle Jurassic of Skye, Scotland. *Transactions of the Royal Society of Edinburgh: Earth Sciences*, 97(1), 25–29. <https://doi.org/10.1017/S0263593300001383>
- Barrett, P. M., Butler, R. J., Edwards, N. P., & Milner, A. R. (2008). Pterosaur distribution in time and space: an atlas. *Zitteliana*, B28, 61–107.
- Barron, A. J. M., Lott, G. K., & Riding, J. B. (2012). Stratigraphic framework for the Middle Jurassic strata of Great Britain and the adjoining continental shelf. *British Geological Survey Research Report, RR/11/06*, 1–177.
- Bennett, S.C. (1993). The ontogeny of *Pteranodon* and other pterosaurs. *Paleobiology*, 19, 92–106.
- Britt, B. B., Dalla Vecchia, F. M., Chure, D. J., Engelmann, G. F., Whiting, M. F., & Scheetz, R. D. (2018). *Caelestiventus hanseni* gen. et sp. nov. extends the desert-dwelling pterosaur record back 65 million years. *Nature Ecology & Evolution* 2:9, 2(9), 1386–1392. <https://doi.org/10.1038/s41559-018-0627-y>
- Butler, R. J., Barrett, P. M., Nowbath, S., & Upchurch, P. (2009). Estimating the effects of sampling biases on pterosaur diversity

- patterns: implications for hypotheses of bird/pterosaur competitive replacement. *Paleobiology*, 35, 432–446.
- Butler, R. J., Benson, R. B. J., & Barrett, P. M. (2013). Pterosaur diversity: untangling the influence of sampling biases, Lagerstätten, and genuine biodiversity signals. *Palaeogeography, Palaeoclimatology, Palaeoecology*, 372, 78–87.
- Cau, A. (2018). The assembly of the avian body plan: a 160-million-year long process. *Bollettino Della Società Paleontologica Italiana*, 57(1), 1–25.
- Cheng, X., Jiang, S., Wang, X., & Kellner, A. W. A. (2017). New anatomical information of the wukongopterid *Kunpengopterus sinensis* Wang et al., 2010 based on a new specimen. *PeerJ*, 5, e4102. DOI 10.7717/peerj.4102.
- Codorniu, L., Carabajal, A. P., Pol, D., Unwin, D., & Rauhut, O. W. M. (2016). A Jurassic pterosaur from Patagonia and the origin of the pterodactyloid neurocranium. *PeerJ*, 4, e2311.
- Cúneo, R., Ramezani, J., Scasso, R., Pol, D., Escapa, I., Zavattieri, A. M., & Bowring, S. A. (2013). High-precision U–Pb geochronology and a new chronostratigraphy for the Cañadón Asfalto Basin, Chubut, central Patagonia: Implications for terrestrial faunal and floral evolution in Jurassic. *Gondwana Research*, 24(3–4), 1267–1275. <https://doi.org/10.1016/j.jgr.2013.01.010>
- Dalla Vecchia, F. M. (2009). Anatomy and systematics of the pterosaur *Carniadactylus* gen. n. *Rosenfeldi* (Dalla Vecchia, 1995). *Rivista Italiana di Paleontologia e stratigrafia*, 115, 159–188.
- Dalla Vecchia, F. M. (2018). Comments on Triassic pterosaurs with a commentary on the “ontogenetic stages” of Kellner (2015) and the validity of *Bergamodactylus wildi*. *Rivista Italiana Di Paleontologia e Stratigrafia*, 124(2), 317–341. <https://doi.org/10.13130/2039-4942/10099>
- Dalla Vecchia, F. M. (2009). The presence of an orbitalantorbital fenestra: further evidence of the anurognathid peculiarity within the Pterosauria. *Rivista Italiana Di Paleontologia e Stratigrafia*, 128(1), 23–42. <https://doi.org/10.54103/2039-4942/16973>
- Davidson, A., & Brown, G. W. (2012). Paraloïd™ B72: practical tips for the vertebrate fossil preparator. *Collection Forum*, 26(1–2), 99–119.
- Dean, C. D., Mannion, P. D., & Butler, R. J. (2016). Preservational bias controls the fossil record of pterosaurs. *Palaeontology*, 59, 225–247.
- Evans, S. E., Barrett, P. M., Hilton, J., Butler, R. J., Jones, M. E. H., Liang, M.-M., Parish, J. C., Rayfield, E. J., Sigogneau-Russell, D., & Underwood, C. J. (2006). The Middle Jurassic vertebrate assemblage of Skye, Scotland. In P. M. Barrett & S. E. Evans (Eds.), *Ninth International Symposium on Mesozoic Terrestrial Ecosystems and Biotas* (pp. 36–39). Natural History Museum, London.
- Fastnacht, M. (2005). The first dsungaripterid pterosaur from the Kimmeridgian of Germany and the biomechanics of pterosaur long bones. *Acta Palaeontologica Polonica*, 50(2), 273–288.
- Galton, P. M. (1981). A rhamphorhynchoid pterosaur from the Upper Jurassic of North America. *Journal of Paleontology*, 55(5), 1117–1122.
- Gao, H.-L., Zhao, Y., Zhang, S.-H., Liu, J., Ye, H., Wang, G.-C., & Liu, J.-M. (2019). Ages of Jurassic volcano-sedimentary strata in the Yanshan Fold-and-Thrust Belt and their implications for the coal-bearing strata of northern China. *International Geology Review*, 61(8), 956–971. <https://doi.org/10.1080/00206814.2018.1481459>
- Goloboff, P. A., & Catalano, S. A. (2016). TNT version 1.5, including a full implementation of phylogenetic morphometrics. *Cladistics*, 32(3), 221–238. <https://doi.org/10.1111/CLA.12160>
- Graham, M., & Allington-Jones, L. (2015). Challenges encountered during acid resin transfer preparation of fossil fish from Monte Bolca, Italy. *Palaeontologia Electronica*, 18.2.4 T, 1–9.
- Harris, J. P., & Hudson, J. D. (1980). Lithostratigraphy of the Great Estuarine Group (Middle Jurassic), Inner Hebrides. *Scottish Journal of Geology*, 16, 231–250.
- Jagielska, N., Challands, T. J., O’Sullivan, M., Ross, D. A., Fraser, N. C., Wilkinson, M., & Brusatte, S. L. (2023). New postcranial remains from the Lealt Shale Formation of the Isle of Skye, Scotland, showcase hidden pterosaur diversity in the Middle Jurassic. *Scottish Journal of Geology*. <https://doi.org/10.1144/SJG2023-001>
- Jagielska, N., O’Sullivan, M., Funston, G. F., Butler, I. B., Challands, T. J., Clark, N. D. L., Fraser, N. C., Penny, A., Ross, D. A., Wilkinson, M., & Brusatte, S. L. (2022). A skeleton from the Middle Jurassic of Scotland illuminates an earlier origin of large pterosaurs. *Current Biology*, 32, 1–17. <https://doi.org/10.1016/j.cub.2022.01.073>
- Kaup, S. S. (1834). Versuch einer Eintheilung der Saugethiere in 6 Stämme und der Amphibien in 6 Ordnung. *Isis von Oken*, 1834, 311–324.
- Lautenschlager, S. (2016). Reconstructing the past: methods and techniques for the digital restoration of fossils. *Royal Society Open Science*, 3, 160342.
- Lautenschlager, S. (2017). From bone to pixel-fossil restoration and reconstruction with digital techniques. *Geology Today*, 33(4), 155–159. <https://doi.org/10.1111/gto.12194>
- Lindsay, W. (1986). The acid technique in vertebrate palaeontology: a review. *Geological Curator*, 4, 455–461.
- Lindsay, W. (1995). A review of the acid technique. In C. Collins (Ed.), *The Care and Conservation of Palaeontological Material* (pp. 95–101). Butterworth-Heinemann.
- Liu, Y.-Q., Kuang, H.-W., Jiang, X.-J., Peng, N., Xu, H., & Sun, H.-Y. (2012). Timing of the earliest known feathered dinosaurs and transitional pterosaurs older than the Jehol Biota. *Palaeogeography, Palaeoclimatology, Palaeoecology*, 323–325, 1–12. <https://doi.org/10.1016/j.palaeo.2012.01.017>
- Lü, J. (2009). A New Non-Pterodactyloid Pterosaur from Qinglong County, Hebei Province of China. *Acta Geologica Sinica*, 83(2), 189–199. <https://doi.org/10.1111/j.1755-6724.2009.00062.x>
- Lü, J., & Fucha, X. (2010). A new pterosaur (Pterosauria) from Middle Jurassic Tiaojishan Formation of western Liaoning, China. *Global Geology*, 13(3/4), 113–118.
- Lü, J., Unwin, D. M., Jin, X., Liu, Y., & Ji, Q. (2010). Evidence for modular evolution in a long-tailed pterosaur with a pterodactyloid skull. *Proceedings of the Royal Society B: Biological Sciences*, 277, 383–389.
- Lü, J., Xu, L., Chang, H., & Zhang, X. (2011). A new darwinopterid pterosaur from the Middle Jurassic of western Liaoning, northeastern China and its ecological implications. *Acta Geologica Sinica - English Edition*, 85(3), 507–514. <https://doi.org/10.1111/j.1755-6724.2011.00444.x>
- O’Sullivan, M., & Martill, D. (2018). Pterosauria of the Great Oolite Group (Middle Jurassic, Bathonian) of Oxfordshire and Gloucestershire, England. *Acta Palaeontologica Polonica*, 63. <https://doi.org/10.4202/app.00490.2018>
- Padian, K. (2008). The Early Jurassic pterosaur *Dorygnathus banthensis* (Theodori, 1830) and the Early Jurassic pterosaur *Campylognathoides* Strand, 1928. *Special Papers in Palaeontology*, 80, 1–107.
- Panciroli, E., Benson, R. B. J., Walsh, S., Butler, R. J., Castro, T. A., Jones, M. E. H., & Evans, S. E. (2020). Diverse vertebrate assemblage of the Kilmaluag Formation (Bathonian, Middle Jurassic) of Skye, Scotland. *Earth and Environmental Science Transactions of the Royal Society of Edinburgh*, 111(3), 135–156.
- Sangster, S. (2021). The osteology of *Dimorphodon macronyx*, a non-pterodactyloid pterosaur from the Lower Jurassic of Dorset, England. *Monographs of the Palaeontographical Society*, 175, 1–48. DOI 10.1080/02693445.2021.2037868
- Sullivan, C., Wang, Y., Hone, D. W. E., Wang, Y., Xu, X., & Zhang, F. (2014). The vertebrates of the Jurassic Daohugou Biota of north-eastern China. *Journal of Vertebrate Paleontology*, 34(2), 243–280. <https://doi.org/10.1080/02724634.2013.787316>
- Tischlinger, H., & Frey, E. (2014). A new pterosaur with mosaic characters of basal and pterodactyloid Pterosauria from the Upper Kimmeridgian of Painten (Upper Palatinate, Germany). *Archaeopteryx*, 31, 1–13.
- Toombs, H. A., & Rixon, A. E. (1959). The Use of Acids in the Preparation of Vertebrate Fossils. *Curator*, 2(4), 304–312.
- Unwin, D. M. (2001). An overview of the pterosaur assemblage from the Cambridge Greensand (Cretaceous) of Eastern England. *Fossil Record*, 4, 189–221.
- Unwin, D. M. (2003). On the phylogeny and evolutionary history of pterosaurs. *Geological Society of London, Special Publications*, 217, 139–190.
- Unwin, D. M. (2005). *The pterosaurs: From deep time*. Pi Press, 352 pp.
- Upchurch, P., Andres, B., Butler, R. J., & Barrett, P. M. (2015). An analysis of pterosaurian biogeography: implications for the evolutionary history and fossil record quality of the first flying vertebrates. *Historical Biology*, 27(6), 697–717. <https://doi.org/10.1080/08912963.2014.939077>
- Vidovic, S. U., & Martill, D. M. (2014). *Pterodactylus scolopaceps* Meyer, 1860 (Pterosauria, Pterodactyloidea) from the Upper

- Jurassic of Bavaria, Germany: The Problem of Cryptic Pterosaur Taxa in Early Ontogeny. *PLoS ONE*, 9(10), e110646. <https://doi.org/10.1371/JOURNAL.PONE.0110646>
- Walker, J. D., & Geissman, J. W. (2022). Geologic Time Scale v. 6.0. Geological Society of America. <https://doi.org/10.1130/2022.CTS006C>
- Wang, X., Jiang, S., Zhang, J., Cheng, X., Yu, X., Li, Y., Wei, G., & Wang, X. (2017). New evidence from China for the nature of the pterosaur evolutionary transition. *Scientific Reports*, 7(1), 42763. <https://doi.org/10.1038/srep42763>
- Wang, X., Kellner, A. W. A., Jiang, S., Cheng, X., Meng, X., & Rodrigues, T. (2010). New long-tailed pterosaurs (Wukongopteridae) from western Liaoning, China. *Anais Da Academia Brasileira de Ciências*, 82(4), 1045–1062. <https://doi.org/10.1590/S0001-37652010000400024>
- Wang, X., Kellner, A. W. A., Jiang, S., & Meng, X. (2009). An unusual long-tailed pterosaur with elongated neck from western Liaoning of China. *Anais Da Academia Brasileira de Ciências*, 81, 793–812.
- Wei, X., Pêgas, R. V., Shen, C., Guo, Y., Ma, W., Sun, D., & Zhou, X. (2021). *Sinomacrops bondei*, a new anurognathid pterosaur from the Jurassic of China and comments on the group. *PeerJ*, 9, e11161. <https://doi.org/10.7717/PEERJ.11161/SUPP-3>
- Wellnhofer P. (1975). Die Rhamphorhynchoidea (Pterosauria) der Oberjura-Plattenkalke Süddeutschlands. I. Allgemeine Skelettmorphologie. *Palaeontographica A*, 148, 1–33.
- Wellnhofer, P. (1978). *Pterosauria*. Handbuch der Paläoherpetologie, 19. Gustav Fischer, Stuttgart, 82 pp.
- Wellnhofer, P. (1991). *The Illustrated Encyclopedia of Pterosaurs* (First Edit). Crescent Books.
- White, S., & Ross, D. (2020). *Jurassic Skye: Dinosaurs and Other Fossils of the Isle of Skye*. Pisces Publications.
- Witton, M. P. (2013). *Pterosaurs: natural history, evolution, anatomy*. Princeton University Press.
- Witton, M. P., O’Sullivan, M., & Martill, D. M. (2015). The relationships of *Cuspicephalus scarfi* Martill and Etches, 2013 and *Normannognathus wellnhoferi* Buffetaut et al., 1998 to other monofenestratan pterosaurs. *Contributions to Zoology*, 84(2), 115–127.
- Xu, X., Zhou, Z., Sullivan, C., Wang, Y., & Dong, R. (2016). An updated review of the Middle-Late Jurassic Yanliao Biota: Chronology, taphonomy, paleontology and paleoecology. *Acta Geologica Sinica (English Edition)*, 90, 2229–2243. DOI 10.1111/1755-6724.13033.
- Zhou, C.-F., & Schoch, R. P. (2011). New material of the non-pterodactyloid pterosaur *Changchengopterus pani* (Lü, 2009) from the Late Jurassic Tiaojishan Formation of western Liaoning. *Neues Jahrbuch für Geologie und Paläontologie, Abhandlungen*, 260, 265–275. DOI 10.1127/0077-7749/2011/0131.
- Zhou, C.-F., Gao, K.-Q., Yi, H., Xue, J., Li, Q., & Fox, R. C. (2017). Earliest filter-feeding pterosaur from the Jurassic of China and ecological evolution of Pterodactyloidea. *Royal Society Open Science*, 4 (2), 160672. <https://doi.org/10.1098/RSOS.160672>
- Zhou, Z., & Wang, Y. (2010). Vertebrate diversity of the Jehol Biota as compared with other lagerstätten. *Science China Earth Sciences*, 53(12), 1894–1907. <https://doi.org/10.1007/s11430-010-4094-9>

Handling Editor: Daniela Schwarz.
Phylogenetics Editor: Pedro Godoy.